**REVIEW****Bismuth and Antimony-based Nanoparticles: New Avenues for Sustainable Catalysis and Environmental Remediation**RADHIKA SHAH¹, MAHIMA CHAUDHARY^{1,*}, MUDIT CHAUCHAN¹, AMAN KUMAR², BHAWANA PANT³ and MOHIT⁴¹Department of Chemistry, School of Applied and Life Science, Uttarakhand University, Dehradun-248007, India²Uttarakhand Institute of Pharmaceutical Science, Uttarakhand University, Dehradun-248007, India³Department of Pharmaceutical Science, DBS Global University, Dehradun-248007, India⁴Department of Chemical Engineering, Thapar Institute of Engineering and Technology, Patiala-147004, India

*Corresponding author: E-mail: mahimachaudhary9292@gmail.com

Received: 27 March 2026

Accepted: 15 June 2026

Published online: 3 July 2026

AJC-22393

Nanostructured bismuth- and antimony-containing photocatalysts have become increasingly popular in photocatalytic applications because of their strong visible-light response and adjustable band-gap energies. Compared with conventional photocatalysts such as TiO₂ and ZnO, Bi-based and Sb-based photocatalysts exhibit broader visible-light absorption and more favourable electronic structures. Their photocatalytic performance can be readily tailored through various engineering strategies, including defect engineering, elemental doping, morphology control and heterojunction construction. This review article summarizes some of the successful uses of Bi- and Sb-based nanostructured semiconductor photocatalysts for the degradation of organic dyes, pharmaceuticals, pesticides and heavy metals from aqueous solutions. Specific examples are provided to demonstrate the influence of morphology variation, oxygen vacancies and the construction of Z-scheme or S-scheme heterojunctions on the enhanced photocatalytic activity of Bi- and Sb-based nanomaterials. Recent developments in synthesis strategies and heterostructure design are also discussed in relation to improved catalytic activity and stability. Current challenges, including photocorrosion, catalyst deactivation, scalability, recyclability, and the potential ecotoxicity of Sb-containing materials, are highlighted, together with future perspectives for the development of sustainable and efficient photocatalytic systems.

Keywords: Bismuth nanoparticles, Antimony nanoparticles, Sustainable catalysis, Environmental remediation, Photocatalysis.**INTRODUCTION**

Rapid industrialization, urbanization and agricultural intensification have substantially increased the discharge of hazardous contaminants, such as dyes, pharmaceuticals, pesticides and heavy metals, into aquatic and terrestrial ecosystems [1-5]. These contaminants exhibit high persistence, bioaccumulation potential and long-term toxicity, posing serious risks to ecosystems and human health. Conventional wastewater treatment techniques including adsorption, coagulation-flocculation, membrane filtration and biological treatment are widely used; however, their practical efficiency is often limited by incomplete mineralisation, secondary sludge formation, membrane fouling and high operational costs [4,5]. Consequently, the development of sustainable and efficient remediation technologies has become an important environmental priority.

Semiconductor photocatalysis has emerged as a promising strategy for pollutant degradation under light irradiation due to its low energy consumption, solar-energy utilisation and efficient contaminant mineralisation [6-10]. Photocatalytic performance is governed by carrier mobility, interfacial charge transfer kinetics, light absorption and long-term structural stability. Conventional photocatalysts such as titanium dioxide (TiO₂), zinc oxide (ZnO), graphitic carbon nitride (g-C₃N₄) and hematite (Fe₂O₃) have been extensively studied owing to their favourable photocatalytic activity, chemical stability and cost-effectiveness. However, their practical application is often constrained by inherent electronic and structural limitations, such as wide band-gap energies, rapid recombination of photo-generated charge carriers and limited visible-light utilization.

TiO₂ and ZnO possess wide band gaps (~3.2-3.3 eV), limiting their photocatalytic response mainly to the ultraviolet

region, which represents only a small fraction of solar radiation [11,12]. ZnO additionally suffers from photocorrosion during prolonged irradiation. Although $g\text{-C}_3\text{N}_4$ exhibits visible-light responsiveness, its photocatalytic activity is hindered by poor conductivity and rapid exciton recombination [13]. Similarly, Fe_2O_3 demonstrates sluggish charge-transfer kinetics and low carrier mobility despite its narrow band gap [14]. These limitations have accelerated the search for visible-light responsive photocatalysts with improved electronic structures and enhanced catalytic stability.

In this context, Bi- and Sb-based nanomaterials have attracted significant attention owing to their tunable electronic structures, layered morphologies, narrow band gaps and efficient visible-light utilisation [6-10,15,16]. Among these materials, BiVO_4 exhibits superior visible-light photocatalytic efficiency compared with TiO_2 since its narrower band gap (~ 2.4 eV) enables efficient solar-light harvesting, while its monoclinic scheelite structure promotes improved carrier migration and interfacial charge transport. Similarly, BiOX materials possess intrinsic internal electric fields that facilitate directional charge separation and suppress electron-hole recombination. The hybridisation of Bi $6s$ and O $2p$ orbitals further enhances visible light absorption capability and photocatalytic performance [7].

Sb-based semiconductors such as Sb_2S_3 and Sb_2O_3 also demonstrate strong visible-light absorption, enhanced conductivity and efficient electron-transport properties, making them promising candidates for photocatalytic and photoelectrochemical applications [7,15]. Unlike TiO_2 and ZnO, Bi-/Sb-based photocatalysts exhibit enhanced activity under visible-light irradiation owing to their narrower band-gap energies [17-22]. Despite these advances, several critical challenges remain, including photocorrosion, catalyst deactivation, metal-ion leaching, limited recyclability and barriers to large-scale implementation.

The catalytic efficiency of Bi-/Sb-based nanomaterials can be further improved through heterojunction engineering, elemental doping, defect modulation and nanocomposite formation. In particular, Type-II and Z-scheme heterojunctions significantly enhance interfacial charge separation and prolong carrier lifetime, thereby improving photocatalytic activity and redox performance [7-10]. Beyond photocatalytic degradation, these materials have also demonstrated considerable potential in hydrogen evolution, CO_2 reduction, antibacterial treatment, sensing applications and wastewater purification.

Bibliometric analysis and research trends: Bibliometric analysis was conducted using the Scopus and Web of Science

databases. Literature retrieval was performed in January 2026 using keywords including ‘ BiVO_4 photocatalyst’, ‘BiOX’, ‘ Sb_2S_3 ’, ‘visible-light photocatalysis’ and ‘environmental remediation’. Only peer-reviewed English-language articles and review papers published between 2014 and 2025 were included (Fig. 1). Duplicate records were removed prior to analysis and keyword co-occurrence mapping was performed using VOSviewer software (Fig. 2).

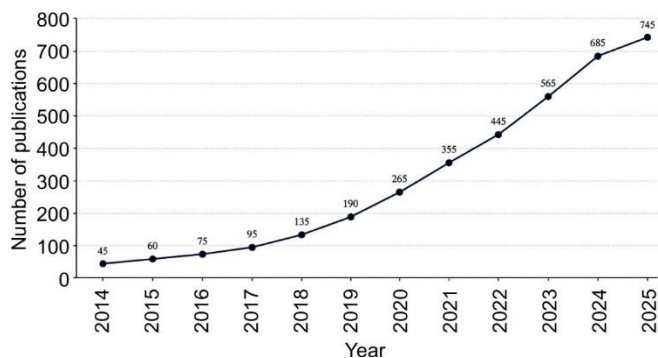


Fig. 1. Annual publication growth of Bi- and Sb-based photocatalytic nanomaterials reported in Scopus and Web of Science databases from 2014-2025

Keyword co-occurrence analysis revealed that major research themes include BiVO_4 heterostructures, BiOX materials, oxygen-vacancy engineering, Z-scheme photocatalysis and Sb_2S_3 -based nanocomposites. Increasing interdisciplinary collaboration and citation impact further emphasize the expanding scientific relevance of these materials in environmental-remediation research.

Among the investigated materials, the photocatalytic activity of BiVO_4 originates from its narrow band gap, efficient interfacial carrier migration and strong visible-light absorption (Table-1). In contrast, TiO_2 remains limited by UV-light responsiveness associated with its wide band gap. Although $g\text{-C}_3\text{N}_4$ exhibits strong optical absorption capability, its photocatalytic efficiency is restricted by poor conductivity and rapid recombination of charge carriers. Similarly, Sb_2S_3 demonstrates excellent light-harvesting capability and carrier mobility; however, photocorrosion and possible Sb-ion leaching remain important concerns for long-term applications. Despite substantial progress, several critical challenges remain unresolved including photocorrosion, catalyst recovery, recyclability, environmental safety and industrial scalability. Therefore, a comprehensive and critical evaluation of Bi-/Sb-based nanomaterials is essential for the rational design of efficient, stable

TABLE-1
BIBLIOMETRIC INDICATORS AND EMERGING RESEARCH TRENDS IN Bi-/Sb-BASED PHOTOCATALYTIC NANOMATERIALS

Parameter	Observation
Publication growth (2014–2025)	Increased from ~42 to >740 publications annually
Major application area	Wastewater remediation and photocatalytic degradation
Most investigated material	BiVO_4
Emerging research trend	Z-scheme and S-scheme heterojunction engineering
Highly recurring keywords	Photocatalysis, BiOX, heterojunction, ROS, visible light
Leading contributing countries	China, India, USA
Major industrial challenge	Catalyst stability and large-scale scalability
Recent focus area	Oxygen-vacancy engineering and multifunctional nanocomposites

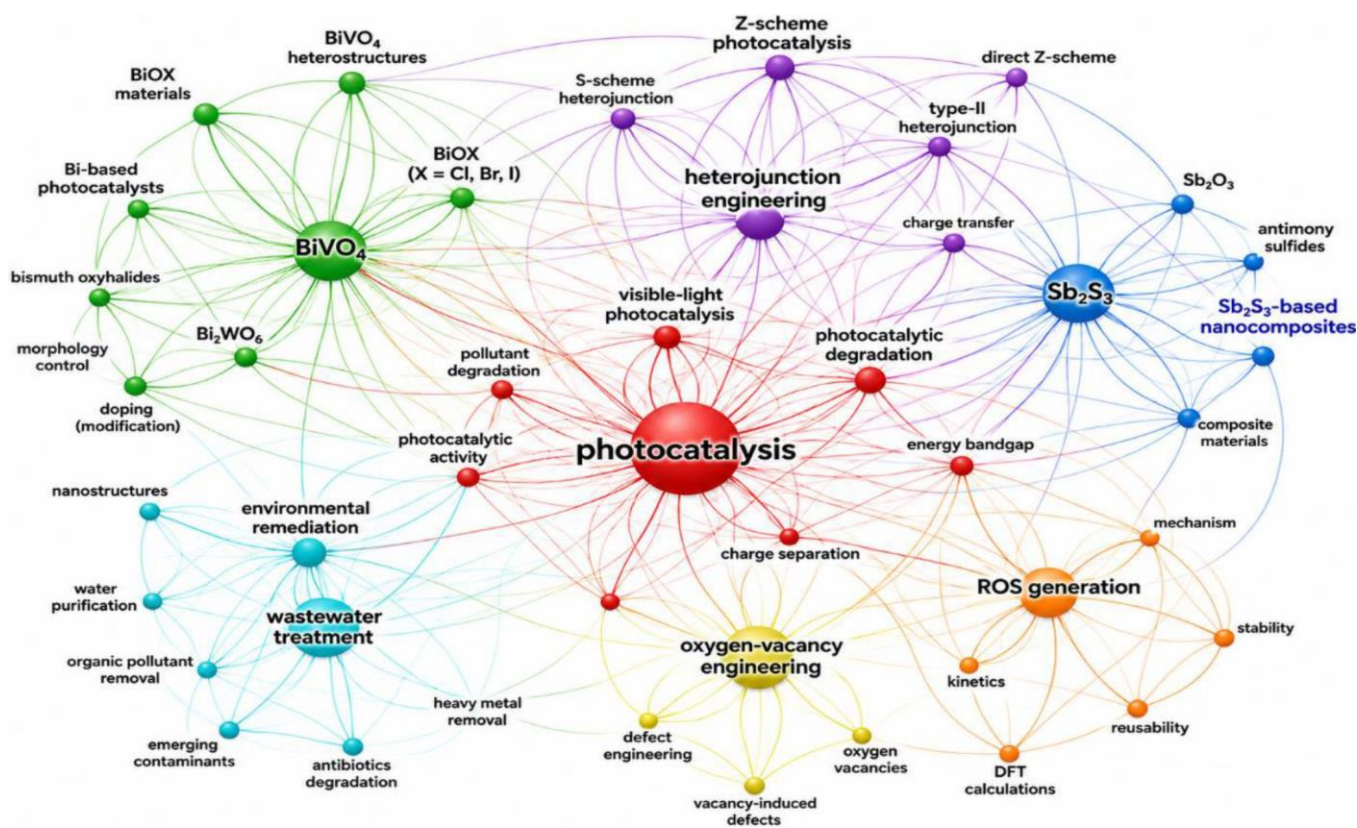


Fig. 2. Keyword co-occurrence network illustrating major research themes in Bi-/Sb-based photocatalytic systems

and sustainable photocatalytic systems for future environmental remediation applications.

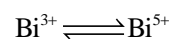
Properties of Bi- and Sb-based nanoparticles: Bi- and Sb-based nanomaterials exhibit distinctive physico-chemical and electronic properties that make them highly promising for photocatalytic, electrochemical, sensing and environmental-remediation applications [23-25]. Their catalytic performance is strongly governed by tunable electronic structures, variable oxidation states, defect chemistry and morphology-dependent charge-transport behaviour. Compared with conventional photocatalysts such as TiO₂, Bi-based materials exhibit enhanced visible-light activity owing to their narrow band-gap energies (typically 1-2 eV) and stereochemically active 6s² lone-pair electrons [26-30]. In contrast, Sb-based nanomaterials possess comparatively higher electrical conductivity and charge-carrier mobility, thereby facilitating rapid interfacial electron transfer and enhanced redox-assisted catalytic activity [31,32].

Physico-chemical properties: Bi- and Sb-based nanoparticles generally crystallize in rhombohedral structures and exhibit tunable semimetallic-to-semiconducting characteristics at the nanoscale [23]. Their high surface-area-to-volume ratios increase the density of catalytically active sites and improve adsorption-desorption kinetics during heterogeneous reactions. Furthermore, nanoscale structural modulation alters the electronic band structure, thereby enhancing visible-light absorption and surface reactivity.

Bi-based nanomaterials, particularly Bi₂O₃ and BiOX systems, contain stereochemically active 6s² lone-pair electrons that induce internal electric polarisation and facilitate directional migration of photogenerated charge carriers [28-30]. As

a result, electron-hole recombination is significantly inhibited, leading to improved charge utilization and enhanced photocatalytic oxidation activity. Layered BiOX structures containing [Bi₂O₂]²⁺ slabs generate intrinsic electric fields that further improve charge separation and interfacial electron-transfer kinetics [26]. In addition, oxygen vacancies introduce localised electronic states that enhance oxygen adsorption and promote reactive oxygen species (ROS) generation during photocatalysis. Hierarchical Bi₂O₃ architectures can exhibit specific surface areas exceeding 50 m² g⁻¹, thereby improving pollutant adsorption and catalytic accessibility [29].

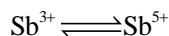
Redox behaviour and oxidation states: The presence of multiple oxidation states, notably the Bi³⁺/Bi⁵⁺ and Sb³⁺/Sb⁵⁺ redox couples, plays a crucial role in enhancing the photocatalytic activity of Bi- and Sb-based nanomaterials by facilitating charge-carrier migration and interfacial redox reactions [33-36]. These reversible valence transitions facilitate rapid electron exchange, accelerate oxidation-reduction pathways and improve charge-carrier separation during photocatalytic reactions.



In Bi-based systems, the reversible Bi³⁺/Bi⁵⁺ transition acts as an efficient electron-transfer mediator that enhances surface redox cycling and ROS generation, including hydroxyl and superoxide radicals [33-36]. Oxygen vacancies further strengthen this mechanism by trapping photogenerated electrons and suppressing electron-hole recombination, thereby improving photocatalytic degradation efficiency and catalytic durability. Controlled defect engineering and heterojunction construction

have therefore emerged as effective strategies for improving visible-light absorption and long-term photocatalytic stability.

Similarly, the defect-rich surface structure and high electrical conductivity of Sb-based nanomaterials promote efficient interfacial electron transfer, thereby enhancing charge-carrier mobility and photocatalytic activity.



The $\text{Sb}^{3+}/\text{Sb}^{5+}$ redox cycle accelerates catalytic oxidation pathways through continuous electron exchange at catalyst interfaces [33-36]. However, excessive oxidation may induce photocorrosion, structural instability and metal-ion leaching, thereby limiting long-term catalytic durability and environmental compatibility.

Structural and morphological features: The catalytic performance of Bi- and Sb-based nanomaterials is strongly dependent on morphology-regulated surface characteristics, crystallographic orientation, porosity and electron-transport pathways rather than merely the existence of different nanostructures [37-39]. Morphological engineering directly influences exposed crystal facets, adsorption capacity, carrier-diffusion pathways and interfacial charge-transfer efficiency. For example, 2D Bi-based nanosheets provide shortened diffusion lengths for photogenerated charge carriers and expose a larger density of catalytically active sites, thereby enhancing visible-light-driven photocatalytic activity [26]. Hierarchical porous architectures provide enhanced light utilisation and pollutant adsorption owing to their high surface areas and multiple light-reflection pathways, while hollow structures facilitate efficient mass transport, increased accessibility of active sites, and superior structural stability during prolonged photocatalytic operation.

In Sb-based systems, anisotropic nanorods and nanoplates facilitate directional electron transport and improve interfacial conductivity [38]. Similarly, Bi-Sb alloy nanocomposites anchored on porous carbon supports demonstrate improved electrical conductivity, electrochemical stability and active-site accessibility, owing to the ability of the conductive matrix to promote efficient electron migration and prevent nanoparticle aggregation [39]. Therefore, rational regulation of morphology, defect chemistry and electronic structure is essential for optimizing the catalytic and photocatalytic performance of Bi- and Sb-based nanomaterials

Environmental compatibility and toxicity considerations: Bi- and Sb-based nanomaterials exhibit distinct toxicity profiles that influence their environmental and biomedical applications. Although Bi-based nanomaterials are widely regarded as comparatively benign owing to their low bioaccumulation tendency and favourable biocompatibility [40], their potential environmental risks cannot be overlooked. Parameters including particle size, morphology, surface characteristics, and dissolution behaviour may significantly affect their environmental fate, long-term stability and ecotoxicological profile.

In contrast, Sb-based nanomaterials raise greater environmental and toxicological concerns owing to their propensity to generate reactive oxygen species, induce oxidative stress, and release metal ions [41]. However, surface modification strategies including PEGylation and polymer-based coatings, can enhance colloidal stability and mitigate potential toxic

effects. Despite these advances, comprehensive ecotoxicological investigations and environmental risk assessments remain necessary to evaluate the long-term safety of both Bi- and Sb-based nanomaterials. From an environmental perspective, current evidence suggests that Bi-based nanomaterials are generally regarded as environmentally more benign than Sb-based counterparts; nevertheless, systematic toxicity assessments are essential to ensure their safe and sustainable implementation in practical applications.

Synthesis methods: Bi- and Sb-based nanomaterials have attracted considerable attention owing to their tunable electronic structures, visible-light responsiveness, morphology dependent photocatalytic activity and effectiveness in environmental remediation [42-48]. The physico-chemical properties of these materials are strongly governed by the synthesis route, which influences particle size, crystallinity, morphology, defect density, optical absorption and charge-transfer characteristics [49-55]. Consequently, a wide range of synthesis strategies, including chemical reduction, hydrothermal/solvothermal processing, microwave-assisted synthesis, electrochemical methods, photochemical approaches and green synthesis, have been explored to optimize photocatalytic performance for wastewater treatment and related environmental applications [56-64].

Among these methods, hydrothermal and solvothermal methods offer excellent crystallinity, phase purity and morphology control, whereas chemical reduction enables rapid synthesis and effective particle-size tuning [42,43,53-55]. Microwave-assisted synthesis provides rapid volumetric heating, shortened reaction times, improved nanoparticle uniformity and enhanced production efficiency [45]. Green synthesis represents an environmentally benign alternative by reducing the use of hazardous chemicals, although reproducibility may be affected by variations in biological precursors [50-52]. Electrochemical and photochemical methods facilitate precise defect engineering and heterostructure fabrication but generally require more sophisticated instrumentation and operational control [55,62-64].

Despite significant advances, no single synthesis route fully satisfies the requirements of structural precision, scalability, reproducibility, cost-effectiveness and environmental sustainability. A comparative assessment of the major synthesis approaches is shown in Table-2. Based on current reports, microwave-assisted synthesis represents a promising approach for large-scale photocatalyst production, offering an effective balance between processing speed, energy efficiency, productivity and material quality [45].

Chemical reduction techniques: Chemical reduction is widely employed for the synthesis of Bi- and Sb-based nanoparticles owing to its operational simplicity, rapid reaction kinetics and ability to produce high-purity nanostructures under relatively mild conditions [46,47]. Common reducing agents include sodium borohydride, hydrazine, D-glucose and Al powder, while stabilizing agents such as polyvinylpyrrolidone (PVP), starch, and glycine are used to prevent agglomeration and enhance colloidal stability [47-49]. The physico-chemical properties of the resulting nanoparticles can be tailored by controlling precursor concentration, pH, reaction temperature and reducing-agent strength, enabling precise regulation of particle size, morphology and crystallinity [48]. Smaller nano-

TABLE-2
COMPARATIVE SYNTHESIS APPROACHES FOR BI- AND Sb-BASED NANOPARTICLES
CONSIDERING SCALABILITY, INDUSTRIAL FEASIBILITY AND MORPHOLOGY CONTROL

Method	Morphology control	Scalability	Cost-effectiveness	Major advantages	Major limitations	Ref.
Chemical reduction	High	Moderate	Moderate	Rapid synthesis, tunable particle size	Toxic reducing agents, agglomeration	[42,47,62]
Green synthesis	Moderate	High	High	Eco-friendly and low toxicity	Poor reproducibility and extract variability	[44,46,50-52]
Hydrothermal/solvothermal	Excellent	Moderate	Moderate	High crystallinity and phase purity	High energy and pressure requirements	[43,53,65]
Microwave-assisted synthesis	High	High	Moderate	Rapid heating and shorter reaction time	Specialised equipment required	[45]
Electrochemical synthesis	Excellent	Moderate	Low	Controlled nanoparticle growth and purity	High operational complexity	[64]
Photochemical synthesis	Moderate	Low	Moderate	Mild reaction conditions and defect engineering	Lower yield and slower synthesis rate	[55,63]

particles generally provide larger specific surface areas and more efficient charge-transfer characteristics, which are beneficial for photocatalytic applications [48,49].

Despite these advantages, chemical-reduction methods face challenges related to the use of hazardous reducing agents, generation of chemical waste and nanoparticle aggregation during scale-up processes [49]. Furthermore, minor variations in reaction parameters can significantly influence particle morphology and crystallinity, affecting reproducibility [47-49]. Although chemical reduction offers rapid synthesis and relatively high product yields compared with many conventional methods, the development of safer reducing agents, environ-

mentally benign solvents and optimized reaction protocols remains essential for improving sustainability and facilitating industrial implementation [42,47].

Green synthesis using plant extracts and biotemplates:

Green synthesis has emerged as an environmentally sustainable alternative for preparing Bi- and Sb-based nanoparticles using plant extracts, microorganisms, algae, fungi and biomolecules as reducing and stabilizing agents (Fig. 3) [50-52]. Natural phytochemicals including flavonoids, polyphenols, citric acid, tannins and ascorbic acid facilitate metal-ion reduction and nanoparticle stabilisation under mild reaction conditions [50,51]. This approach minimizes toxic chemical

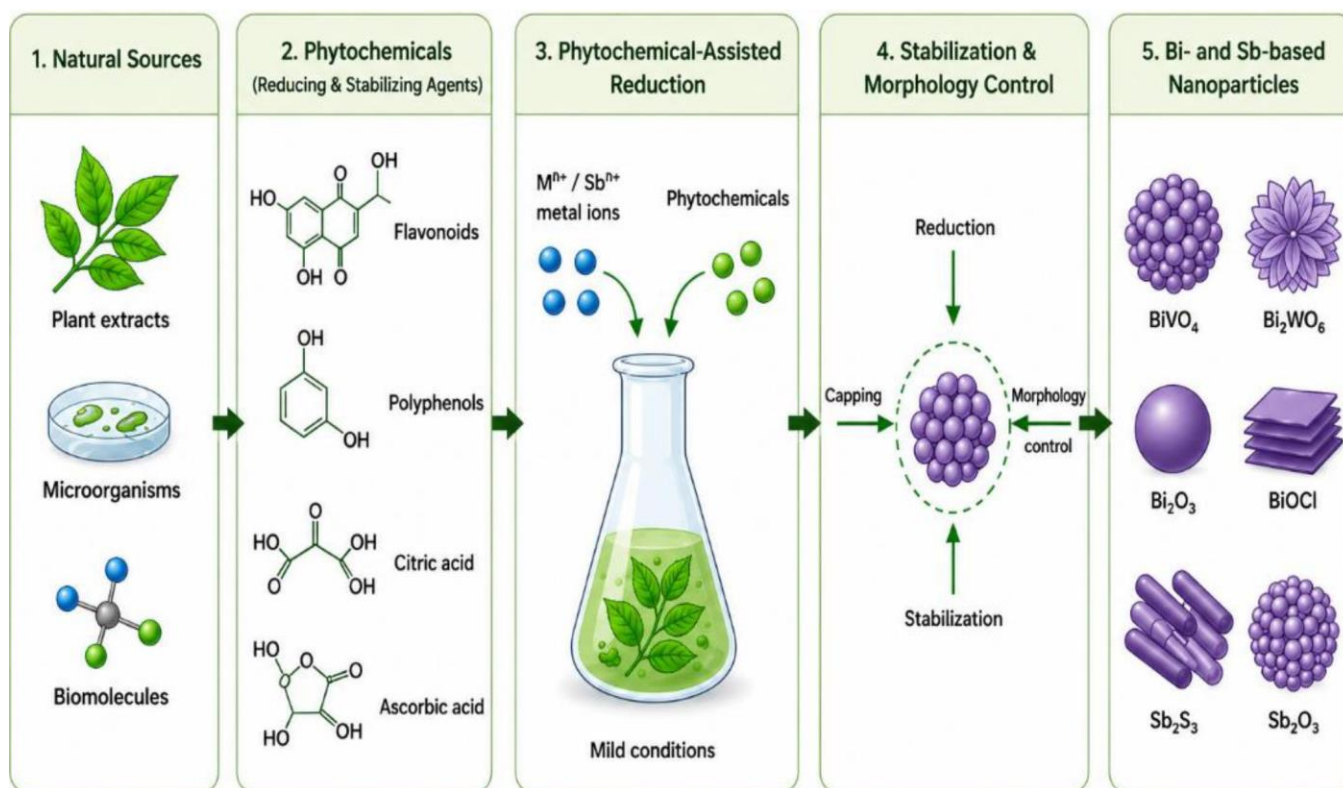


Fig. 3. Schematic illustration of plant-mediated green synthesis pathways for Bi- and Sb-based nanoparticles showing phytochemical-assisted reduction, stabilisation and morphology control

consumption, lowers environmental risk and improves biocompatibility, making green synthesis attractive for environmental and biomedical applications [50-52].

However, reproducibility remains a significant challenge since the composition of plant extracts can vary with species, geographical origin, seasonal factors, cultivation conditions, and extraction protocols [51,52]. Such variations may substantially influence nanoparticle size, crystallinity, morphology and photocatalytic performance [51]. In addition, ensuring consistent phytochemical composition during large-scale production remains challenging, thereby hindering industrial scalability [52]. Although green synthesis offers outstanding advantages, including reduced toxicity and lower energy consumption, the standardization of biological precursors and extraction procedures remains essential for reliable large-scale implementation.

Hydrothermal synthesis offers excellent phase purity, crystallinity and defect control, which contribute to enhanced visible-light absorption and efficient charge-carrier separation [53]. However, its industrial application is constrained by prolonged reaction times, high energy requirements, pressure-related safety concerns and the need for specialized high-pressure autoclaves [54]. Microwave-assisted hydrothermal synthesis addresses several of these limitations by enabling rapid and uniform heating, resulting in shorter reaction times, improved nanoparticle uniformity and reduced energy consumption [45]. Consequently, microwave-assisted approaches generally provide higher productivity and greater potential for scale-up than conventional hydrothermal methods.

Electrochemical and photochemical routes: Electrochemical and photochemical synthetic methods enable the

controlled fabrication of Bi- and Sb-based nanomaterials through electron-transfer-driven reduction processes [55,62] (Fig. 4). In electrochemical synthesis, metal ions are reduced at electrode surfaces under an applied potential, allowing precise control over nucleation, growth, particle thickness and surface composition [62,64]. Photochemical synthesis, in contrast, relies on light-induced reduction or decomposition of precursor species, facilitating nanoparticle formation under relatively mild conditions [55]. These approaches offer several advantages, including high product purity, reduced solvent consumption, precise defect engineering and controlled heterostructure fabrication [62-64]. The photochemical methods are particularly effective for generating oxygen vacancies and surface defects, which enhance visible-light absorption, charge carrier separation and ROS production during photocatalysis [63]. Despite these benefits, photochemical synthesis is often limited by relatively low yields and slower reaction rates, whereas electrochemical methods require sophisticated instrumentation, electrode optimization and higher operational costs [62-64]. As a result, although both techniques provide excellent structural and compositional control, their large-scale industrial implementation remains challenging.

Controlled size and shape engineering: The photocatalytic efficiency of Bi- and Sb-based nanomaterials strongly depends on particle size, morphology, surface defects, exposed crystal facets and band structure [64-67]. Controlled size and shape engineering can be achieved by adjusting surfactant concentration, solvent composition, precursor ratio, reaction temperature and synthesis duration [64]. Nanoplates, nanorods, nanosheets and hierarchical architectures generally provide larger active surface area, shorter diffusion pathways, enhanced

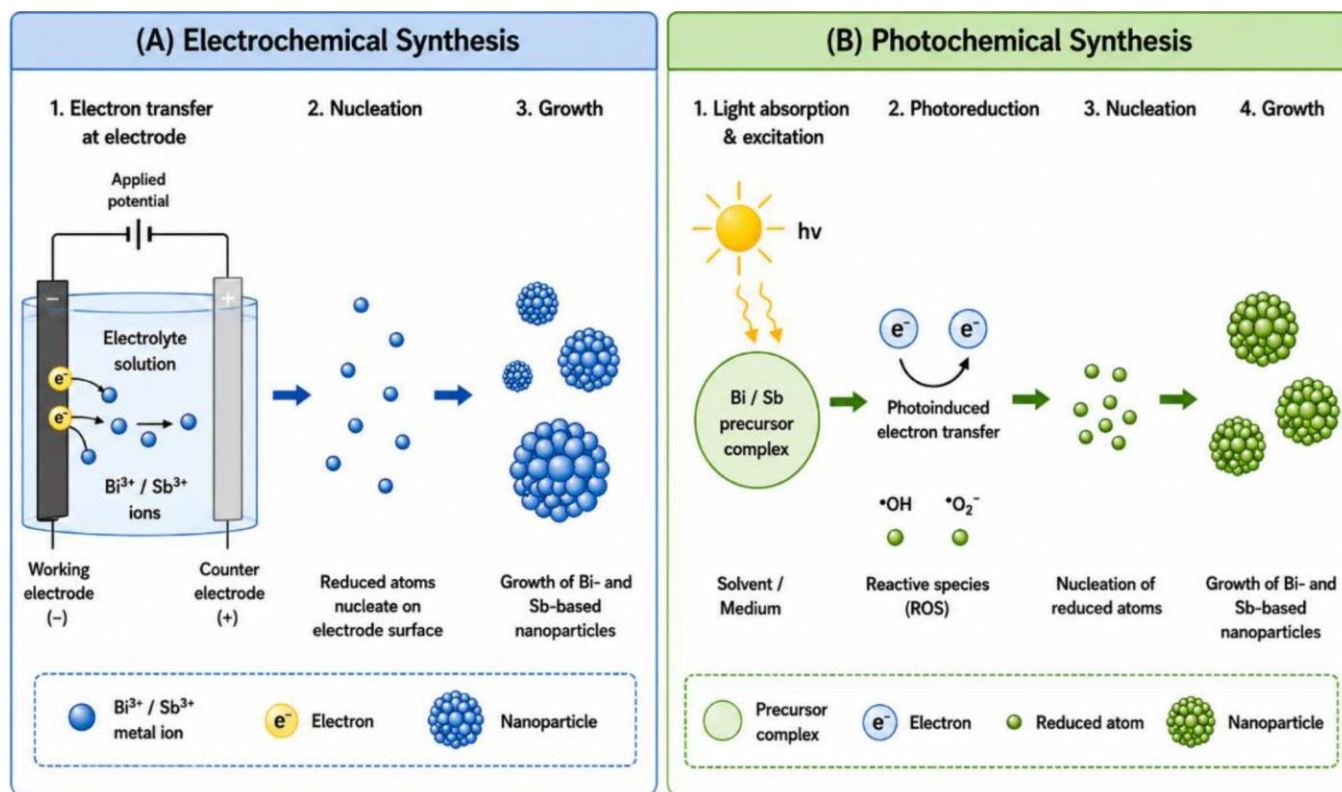


Fig. 4. Electrochemical and photochemical synthesis mechanisms showing electron transfer, nucleation and nanoparticle growth

visible-light absorption and improved charge-transfer efficiency compared with bulk materials [66,67].

Particle-size reduction can induce band-gap modification through quantum-confinement effects, thereby improving visible-light utilisation and suppressing electron-hole recombination [66]. Similarly, anisotropic nanostructures such as nanowires and nanosheets facilitate directional electron transport and enhance interfacial charge migration [67]. The morphology-controlled Bi-Sb heterostructures additionally improve reactive oxygen species generation and pollutant degradation efficiency during photocatalysis [65]. Therefore, precise morphology engineering remains a critical strategy for optimizing environmental-remediation performance and wastewater-treatment efficiency.

No currently available synthesis method simultaneously fulfills all the requirements for industrial-scale photocatalyst production including scalability, reproducibility, energy efficiency, structural precision and environmental sustainability. Hydrothermal and solvothermal approaches provide excellent crystallinity and morphology control but remain limited by high energy demands and scalability challenges [53,54]. Microwave-assisted synthesis offers a favourable balance between production efficiency, scalability and material quality, whereas green synthesis minimises environmental impact through the use of benign reagents and conditions. Electrochemical and photochemical methods are particularly effective for defect engineering and heterostructure construction, although their practical implementation is constrained by lower throughput and greater operational complexity [55,62-64]. Continued efforts toward hybrid, low-energy and sustainable synthesis platforms are expected to advance the large-scale manufacturing and commercial application of Bi- and Sb-based photocatalysts.

Characterisation techniques: Comprehensive characterisation is essential for establishing correlations between the structural, optical and electronic properties of Bi- and Sb-based nanomaterials and their photocatalytic performance. X-ray diffraction (XRD) is widely employed to determine crystal structure, phase composition, crystallinity and heterojunction formation, while Fourier-transform infrared spectroscopy (FT-IR) is used to identify surface functional groups and chemical bonding characteristics [47,56,60].

Scanning electron microscopy (SEM) and transmission electron microscopy (TEM/HRTEM) provide detailed information on morphology, particle size, lattice structure and interfacial features that influence light harvesting and charge transport [7,14,61]. X-ray photoelectron spectroscopy (XPS) is extensively used to investigate elemental composition, oxidation states, surface chemistry and defect characteristics, particularly oxygen vacancies that affect visible-light absorption and photocatalytic activity [57].

Optical and charge-transfer properties are commonly evaluated using UV-Vis diffuse reflectance spectroscopy (UV-Vis DRS), photoluminescence (PL) spectroscopy, electrochemical impedance spectroscopy (EIS) and photocurrent measurements. These techniques provide valuable insights into light-absorption behaviour, band-gap characteristics, charge-carrier recombination and interfacial electron-transfer processes [58,59,61,62]. Recent advances in *in situ* and time-resolved

characterisation techniques, including *in situ* XPS, *in situ* FTIR, time-resolved PL and transient absorption spectroscopy, have enabled direct investigation of reaction intermediates, carrier dynamics, and photocatalytic mechanisms under operating conditions. Such approaches provide deeper insight into structure-property-activity relationships and facilitate the rational design of highly efficient Bi- and Sb-based photocatalysts for environmental remediation.

Various applications of Bi and Sb nanoparticles: Bi- and Sb-based nanomaterials have attracted considerable attention in photocatalysis and environmental remediation owing to their tunable electronic structures, strong visible-light responsiveness, favourable redox properties, and relatively low toxicity. Bi-based nanomaterials have demonstrated excellent photocatalytic performance for the degradation of a wide range of environmental pollutants, while also exhibiting antibiofilm and antibacterial activities that may contribute to multifunctional environmental applications [68]. Similarly, Sb-based nanomaterials possess favourable electrical conductivity, tunable morphologies and good electrochemical stability, making them promising candidates for photocatalytic and photoelectrochemical systems [69].

Compared with many conventional photocatalysts, Bi- and Sb-based materials offer advantages such as efficient visible-light utilization, tunable electronic properties, relatively low cost, and the availability of constituent elements. However, challenges including photocorrosion, catalyst deactivation, limited long-term stability, material recovery and large-scale implementation continue to hinder their practical application. Addressing these limitations through advanced material design, heterostructure engineering and sustainable synthesis strategies remains essential for the development of efficient and durable photocatalytic systems.

Catalytic applications: Bi- and Sb-based nanomaterials exhibit excellent catalytic performance owing to their tunable oxidation states, oxygen-vacancy-rich surfaces, narrow band-gap energies, and efficient visible-light absorption characteristics. These materials have been extensively investigated for photocatalysis, electrocatalysis, water splitting, selective redox reactions, and environmental remediation applications [70].

Bi-based nanomaterials demonstrate high catalytic efficiency in the degradation of organic pollutants and the remediation of toxic metal contaminants due to their strong visible light responsiveness, favourable electronic structures and high surface reactivity [71]. Sb-based materials have also attracted interest as catalytic and photoelectrochemical materials owing to their good electrical conductivity, structural stability and efficient charge-transport properties for example, antimony selenide (Sb_2Se_3) [72]. The catalytic activity of both Bi- and Sb-based systems is strongly influenced by band-structure engineering, interfacial charge-transfer processes, oxygen-vacancy-mediated charge separation and defect-induced active sites. Furthermore, heterojunction construction effectively suppresses electron-hole recombination and promotes charge carrier migration, thereby enhancing catalytic performance. Compared with noble-metal-based catalysts (Pt- and Pd-), Bi- and Sb-based materials offer advantages in terms of lower cost, greater elemental abundance and reduced reliance on critical raw materials. These attributes, combined with their

favourable visible-light-driven catalytic properties, make them promising candidates for sustainable wastewater-treatment and environmental-remediation technologies.

Role in oxidation and reduction reactions: Bi- and Sb-based nanomaterials exhibit excellent catalytic performance owing to their multiple oxidation states ($\text{Bi}^{3+}/\text{Bi}^{5+}$ and $\text{Sb}^{3+}/\text{Sb}^{5+}$), favourable electronic structures and efficient interfacial charge-transfer characteristics [73]. In photocatalytic oxidation processes, materials such as Bi_2O_3 and BiVO_4 generate ROS ($\cdot\text{OH}$ and $\cdot\text{O}_2^-$) under visible-light irradiation, enabling the degradation of a wide range of organic contaminants, including phenols, antibiotics and aromatic pollutants [74]. Bi_2O_3 nanoparticles, for example, have demonstrated high efficiency in the degradation of tetracycline and bisphenol A under mild operating conditions.

Sb-based materials, including Sb_2O_3 , Sb_2S_3 and Sb-modified semiconductors, have also shown promising catalytic activity owing to their enhanced charge-transfer properties and oxygen-activation capability [75]. In environmental remediation, Sb_2S_3 nanostructures have been reported to facilitate the reduction of toxic Cr(VI) to the less harmful Cr(III) form in aqueous systems, highlighting their potential for heavy-metal remediation.

The enhanced catalytic activity of Bi- and Sb-based systems is primarily attributed to efficient charge transport, oxygen vacancy-mediated charge separation and defect-induced active sites that promote interfacial redox reactions. However, catalyst deactivation resulting from surface fouling, photocorrosion and gradual oxidation remains a challenge for long-term operation and repeated catalytic cycles.

Photocatalytic activities: Bi- and Sb-based nanomaterials have emerged as promising visible-light-responsive photocatalysts for the degradation of dyes, pharmaceuticals, pesticides, antibiotics and other emerging contaminants. Materials such as Bi_2O_3 , Bi_2WO_6 , BiVO_4 and BiOX ($X = \text{Cl}, \text{Br}, \text{I}$) and Sb_2S_3 possess relatively narrow band-gap energies and favourable electronic structures that promote visible-light absorption and photocatalytic activity [76,77]. Morphology engineering through the fabrication of nanosheets, nanoflowers and hierarchical architectures further enhances surface area, active-site accessibility and charge-transfer efficiency.

Among these materials, BiVO_4 has received particular attention due to its strong visible-light response, suitable band edge positions and favourable charge-transport characteristics. Compared with conventional TiO_2 , BiVO_4 exhibits superior visible-light utilization owing to its narrower band-gap energy, although its performance remains limited by short carrier diffusion lengths and moderate photostability [11,78]. Similarly, BiOX and Sb_2S_3 photocatalysts have demonstrated excellent photocatalytic activity due to their efficient charge transport and favourable band structures.

The construction of heterojunctions represents one of the most effective strategies for enhancing photocatalytic performance. In particular, Z-scheme and S-scheme heterostructures facilitate efficient charge separation while preserving strong redox capability, thereby promoting reactive oxygen species generation and pollutant degradation [77,79]. In addition, Sb incorporation into Bi-based photocatalysts can improve visible light harvesting, electron-transfer kinetics and defect-assisted

charge separation through band-structure modulation and oxygen-vacancy engineering.

Photocatalytic performance is commonly evaluated using parameters such as apparent quantum yield, pseudo-first-order kinetic constants and mineralisation efficiency. Representative heterojunction systems including $\text{BiVO}_4/g\text{-C}_3\text{N}_4$ composites, have demonstrated substantially enhanced photocatalytic activity compared with pristine photocatalysts, highlighting the effectiveness of heterostructure engineering in improving charge-carrier utilization and degradation efficiency.

Despite these advances, challenges including charge-carrier recombination, photocorrosion, metal-ion leaching, limited recyclability and reduced performance in complex wastewater matrices continue to restrict large-scale implementation. Further progress is expected through the development of advanced heterostructures, cocatalyst integration, defect engineering, surface passivation and long-term stability optimization, which are essential for the practical deployment of Bi- and Sb-based photocatalysts in sustainable wastewater-treatment technologies [76-78]. A comparative analysis of conventional and Bi-/Sb-based photocatalysts for environmental remediation is shown in Table-3.

Electrocatalysis: Bi- and Sb-based nanomaterials have also attracted interest as electrocatalysts for oxygen reduction and hydrogen evolution reactions attributed to their favourable electronic structures, tunable surface chemistry and relatively low cost [80-83]. Bi-based catalysts can selectively promote the two-electron oxygen reduction pathway for H_2O_2 generation, while Bi, Sb, Bi_2S_3 and Sb_2S_3 nanostructures have been investigated as non-noble metal electrocatalysts for hydrogen evolution in both acidic and alkaline media [80,81]. Their electrocatalytic performance can be further enhanced through heterostructure construction, defect engineering, oxygen vacancy generation and integration with conductive carbon supports, which improve charge transport and increase the density of active sites [83]. Despite these advances, their catalytic activity and long-term durability generally remain inferior to those of state-of-the-art Pt-based electrocatalysts, particularly under prolonged operation and high current densities.

In organic transformations: Bi- and Sb-based nanomaterials have gained considerable attention in organic synthesis owing to their Lewis acidity, catalytic selectivity and recyclability. Bi(III)-based catalysts have been widely employed in Friedel-Crafts acylation, aldol condensation, allylation and oxidation reactions under relatively mild conditions [84]. In addition, Bi nanoparticles supported on silica or carbon have demonstrated good catalytic activity and reusability in Suzuki-Miyaura and Heck coupling reactions, affording high product yields [85].

Bi and Bi-Sb alloy nanomaterials have also shown promising performance in selective hydrogenation processes particularly the conversion of alkynes to alkenes, carbonyl compounds to alcohols and nitro compounds to amines [86]. Their favourable hydrogen-activation characteristics enhance chemoselectivity while minimizing undesired over-reduction reactions [87]. Compared with conventional Pd-based catalysts, Bi-based systems offer advantages in terms of lower cost, reduced susceptibility to sulphur poisoning and improved

TABLE-3
COMPARATIVE ANALYSIS OF CONVENTIONAL AND Bi-/Sb-BASED
PHOTOCATALYSTS FOR ENVIRONMENTAL REMEDIATION

Material	Band gap (eV)	Light source	Photocatalytic performance	Stability/recyclability	Key limitation	Ref.
TiO ₂	3.0–3.2	UV light	High degradation and H ₂ production efficiency	Excellent long-term stability and recyclability	Limited visible-light response	[11]
ZnO	3.2–3.3	UV light	Good photocatalytic activity	Moderate stability	Photocorrosion under prolonged irradiation	[11]
g-C ₃ N ₄	~2.7	Visible light	Moderate visible-light activity	Good thermal stability	Rapid charge recombination	[79]
Fe ₂ O ₃	~2.1	Visible light	Moderate photocatalytic efficiency	Poor conductivity limits performance	Short carrier diffusion length	[79]
BiVO ₄	~2.4	Visible light	High dye degradation, water splitting and mineralisation efficiency	Moderate recyclability	Carrier recombination and photocorrosion	[78]
BiOX (Cl, Br, I)	1.8–3.4	Visible light	Rapid dye degradation and ROS generation	Good structural stability	Limited quantum efficiency	[77]
Sb ₂ S ₃	1.7–1.8	Visible light	Enhanced charge transfer and pollutant degradation	Moderate stability	Toxicity and long-term stability concerns	[77]

sustainability, although their reaction rates may be comparatively lower under certain industrial operating conditions.

Comparison with traditional catalysts: Compared with conventional noble-metal catalysts such as Pt, Pd and Ag, Bi- and Sb-based catalysts offer several advantages, notably lower cost, greater elemental abundance, improved environmental compatibility and efficient visible-light responsiveness [88]. Although noble-metal catalysts generally exhibit superior intrinsic catalytic activity and long-term operational stability, Bi- and Sb-based systems often achieve comparable performance in visible-light-driven photocatalytic and selective reduction processes while substantially reducing material costs [89].

Bi-based catalysts additionally demonstrate enhanced resistance to sulphur and halide poisoning relative to Pt-based counterparts, making them attractive for operation in complex wastewater-treatment environments [90]. Furthermore, the comparatively low toxicity of many Bi-containing compounds supports their potential for sustainable catalytic applications. From an industrial perspective, catalyst durability, recyclability and economic feasibility remain key considerations. While Pt- and Pd-based catalysts provide excellent catalytic efficiency and stability, their widespread deployment is constrained by high cost and limited availability. In contrast, Bi- and Sb-based catalysts are relatively inexpensive and can be synthesized using diverse, scalable approaches. However, challenges such as photocorrosion, gradual catalyst deactivation and moderate long-term stability continue to limit practical implementation. Accordingly, advances in heterojunction construction, defect engineering, cocatalyst incorporation and surface passivation remain essential for enhancing durability and facilitating large-scale application [91]. Current advances underscore the potential of Bi- and Sb-based nanomaterials as sustainable alternatives for visible-light-driven catalysis and advanced wastewater-remediation technologies.

Environmental remediation potential: Bi- and Sb-based nanomaterials have demonstrated considerable potential for environmental remediation applications [92]. These materials are highly effective in the removal of organic contaminants, such as dyes, pesticides, pharmaceuticals and phenolic comp-

ounds, as well as toxic heavy metals, including As, Cr and Pb, through visible-light-driven photocatalytic degradation, adsorption and redox-mediated remediation processes [93]. In addition, their antimicrobial properties have attracted interest for wastewater treatment and environmental sanitation applications.

Removal of organic pollutants: Bi- and Sb-based nanomaterials have demonstrated high efficiency in the removal of organic contaminants such as dyes, pesticides, antibiotics, and phenolic compounds, through visible-light-driven photocatalytic degradation and adsorption processes [94-99]. Bi-containing photocatalysts such as Bi₂O₃, BiVO₄, Bi₂WO₆ and BiOX (X = Cl, Br, I), exhibit excellent photocatalytic performance under visible-light irradiation owing to their narrow band-gap energies, efficient charge separation and strong ROS generation [94-96]. These materials have been successfully applied for the degradation of textile dyes, pharmaceuticals and phenolic pollutants, often achieving high degradation and mineralization efficiencies under mild operating conditions.

Sb₂S₃ nanostructures, Sb-doped Bi₂O₃ and Bi-Sb based composite photocatalysts further enhance pollutant removal through improved visible-light harvesting, accelerated charge transfer and suppressed electron-hole recombination [97-99]. In particular, heterojunction construction, oxygen-vacancy engineering, and elemental doping have emerged as effective strategies for improving photocatalytic activity and stability. Composite systems such as BiVO₄/g-C₃N₄ and Bi-Sb/carbon materials benefit from synergistic adsorption-photocatalysis effects, resulting in enhanced degradation performance and broader applicability toward persistent organic pollutants [97-99]. Table-4 provides a comparative assessment of representative Bi- and Sb-based photocatalysts, highlighting pollutant degradation performance, operational conditions, reusability, and the major advantages and limitations of each system.

Despite these advances, challenges related to photocorrosion, structural degradation, metal-ion leaching, pH-dependent stability and catalyst recovery continue to limit practical implementation. Additional concerns regarding the potential ecotoxicity of Sb-containing materials and the comp-

TABLE-4
COMPARATIVE PHOTOCATALYTIC PERFORMANCE OF Bi- AND
Sb-BASED NANOMATERIALS FOR WASTEWATER TREATMENT

Photocatalyst	Target pollutant	Mechanism	Reusability	Major advantages	Practical limitations	Ref.
Bi ₂ O ₃ hierarchical nanostructures	Rhodamine B	Photocatalytic oxidation	5 cycles	Strong visible-light absorption	Structural instability during prolonged use	[100]
BiVO ₄ heterojunctions	Ciprofloxacin	ROS-mediated degradation	5 cycles	Efficient charge separation and narrow bandgap	Slow H ₂ evolution kinetics	[101]
Bi ₂ WO ₆ nanosheets	Methylene Blue	[•] OH/ [•] O ₂ ⁻ radical attack	4 cycles	High visible-light photoresponse	Moderate recyclability	[102]
BiOBr nanosheets	Textile dyes	Surface photocatalysis	5 cycles	Tunable band structure	Sensitive synthesis conditions	[103]
Sb ₂ S ₃ nanorods	Atrazine	Electron–hole degradation	3 cycles	Improved charge transport	Possible Sb toxicity	[104]
Sb-doped Bi ₂ O ₃	Phenolic compounds	Enhanced ROS generation	5 cycles	Improved visible-light activity	Dopant optimisation required	[105]
Bi–Sb/Carbon composite	Mixed dye pollutants	Adsorption-assisted photocatalysis	5 cycles	High conductivity and surface area	Complex synthesis route	[106]
Oxygen-vacancy- rich Bi ₂ O ₃	Methyl orange	Vacancy-mediated photocatalysis	4 cycles	Enhanced charge separation	Defect-induced instability	[107]
BiVO ₄ /g-C ₃ N ₄ Z- scheme	Tetracycline	Z-scheme charge transfer	5 cycles	Superior ROS generation	Multi-step synthesis	[108]
Bi ₂ WO ₆ nanoflowers	Congo Red	Radical oxidation	4 cycles	Large surface area	Poor acidic stability	[109]
BiOI microspheres	Reactive Black 5	Visible-light photocatalysis	5 cycles	Rapid degradation efficiency	Photocorrosion risk	[110]
Sb ₂ S ₃ /TiO ₂ composite	Chlorpyrifos	Heterojunction-assisted degradation	4 cycles	Reduced charge recombination	Instability at high pH	[111]
Sb-doped BiVO ₄	Pharmaceutical residues	ROS-assisted oxidation	5 cycles	Tunable bandgap	Metal-ion leaching risk	[112]
Bi–Sb alloy nanoparticles	Industrial dye mixtures	Synergistic adsorption– photocatalysis	6 cycles	Enhanced electron mobility	Expensive alloy synthesis	[87]

lexity of multistep synthesis processes must also be addressed. Consequently, future research should prioritize the development of durable, environmentally compatible and economically viable Bi- and Sb-based photocatalysts for large-scale wastewater-remediation applications.

Heavy metal adsorption and reduction: Heavy metals such as arsenic (As), chromium (Cr), lead (Pb), cadmium (Cd) and mercury (Hg) are persistent environmental pollutants that require efficient remediation owing to their toxicity, non-biodegradability and tendency to accumulate in ecosystems. Bi- and Sb-based nanomaterials have emerged as promising candidates for heavy-metal remediation through adsorption, surface complexation and redox-mediated transformation mechanisms. Bismuth oxide and bismuth oxychloride nanosheets exhibit high affinity toward As(III) and As(V) species through strong surface complexation at Bi–O active sites [18]. Metallic Bi nanoparticles can facilitate the reduction of toxic Cr(VI) to the less harmful Cr(III) form under near-neutral conditions, whereas Bi–Fe and Bi–Sb composites have demonstrated effective simultaneous removal of Pb(II) and Cd(II) through electrostatic interactions and surface precipitation processes [113,114]. Similarly, antimony oxide and antimony sulphide nanomaterials display strong adsorption capacities toward Hg(II) and Pb(II) ions. The superior remediation performance of these materials is attributed to their high specific surface area, tunable surface chemistry and abundance of

redox-active sites, which promote efficient contaminant capture and transformation compared with many conventional adsorbents [115].

Application in wastewater treatment: Bi- and Sb-based nanomaterials are increasingly being explored for the wastewater-treatment applications owing to their visible-light driven photocatalytic activity, chemical stability and reusability. Photocatalytic reactors incorporating immobilized BiVO₄ and Bi₂WO₆ have demonstrated effective degradation of diverse pollutant mixtures, including dyes, pharmaceuticals and heavy metals, under solar or visible-light irradiation [116]. In membrane based treatment systems, Sb₂S₃-modified membranes exhibit enhanced adsorption performance and improved anti-fouling properties, supporting their application in advanced wastewater-treatment processes. Pilot-scale BiVO₄ photocatalytic systems have also shown efficient treatment of textile effluents while generating substantially lower sludge volumes than conventional coagulation-based methods [117].

The practical applicability of these materials is further supported by their stability over a broad pH range and their ability to maintain catalytic performance during repeated operation cycles [118,119]. These characteristics make Bi- and Sb-based nanomaterials promising candidates for integration into fixed-bed, fluidized-bed, and other continuous-flow wastewater treatment systems. Nevertheless, challenges associated with photocorrosion, catalyst recovery, long-term durability,

and large-scale process optimization must be addressed to facilitate widespread industrial implementation [118,119].

Antimicrobial and anti-biofouling properties: Bi-based nanomaterials also exhibit notable antimicrobial properties, making them attractive for water-treatment, membrane protection and antibiofouling applications [120]. Bi₂O₃ and Bi-based heterostructures can generate ROS under visible light irradiation, leading to effective inactivation of pathogenic microorganisms, including *E. coli* and *S. aureus*, as well as certain viruses. In addition, Bi-nanoparticles and bismuth sulphide nanomaterials have demonstrated strong antibacterial activity and the ability to inhibit biofilm formation, thereby reducing microbial colonization on treatment surfaces.

Similarly, Sb₂S₃ and Sb-doped materials exhibit antimicrobial activity through a combination of oxidative-stress induction and controlled release of Sb³⁺ ions. These properties contribute to reduced biofouling, improved membrane performance, and enhanced operational stability in filtration and wastewater-treatment systems. Consequently, Bi- and Sb-based nanomaterials offer promising opportunities for the development of multifunctional treatment technologies for the pollutant removal with antimicrobial protection.

Biodegradability and eco-friendliness: Bismuth-based nanomaterials generally exhibit lower toxicity and improved environmental compatibility than conventional heavy metal photocatalysts, owing to their minimal leaching and negligible ecotoxicological impact on aquatic organisms [19]. Although antimony-based materials require careful handling due to their relatively higher toxicity, strategies such as surface passivation and controlled release can effectively reduce associated risks [121]. Their abundance, recyclability and reduced dependence on precious metals enhance resource sustainability while minimising environmental impacts related to mining

and secondary pollution, making Bi- and Sb-based materials promising candidates for long-term sustainable photocatalytic and electrocatalytic environmental remediation [122,123].

Mechanistic insights: Under visible-light irradiation, both Bi- and Sb-based photocatalysts generate photoexcited electron-hole pairs that initiate redox reactions through the formation of reactive oxygen species (ROS), including superoxide radicals ($\cdot\text{O}_2^-$), hydroxyl radicals ($\cdot\text{OH}$) and singlet oxygen ($^1\text{O}_2$). Photocatalytic performance is primarily governed by efficient pollutant adsorption, rapid charge separation and migration and suppressed electron-hole recombination. Surface oxygen vacancies, exposed crystal facets and defect sites enhance these processes by providing active adsorption sites and facilitating interfacial charge transfer, thereby accelerating photocatalytic degradation [124].

Photocatalytic mechanisms: Bi- and Sb-based nanomaterials exhibit excellent visible-light-driven photocatalytic activity owing to their narrow band gaps, suitable band-edge positions and efficient generation of reactive oxygen species (ROS), which facilitate the degradation and mineralization of organic contaminants. Upon visible-light irradiation, electrons are excited from the valence band (VB) to the conduction band (CB), generating photogenerated electron-hole (e^-/h^+) pairs. In Bi-based photocatalysts, including Bi₂O₃, BiVO₄ and BiOX, hybridization between the Bi 6s and O 2p orbitals elevates the VB maximum and narrows the band gap (≈ 1.8 -2.8 eV), thereby enhancing visible-light absorption and solar energy utilization [88]. The photogenerated holes oxidize adsorbed H₂O or OH⁻ to produce hydroxyl radicals ($\cdot\text{OH}$), whereas CB electrons reduce dissolved O₂ to generate superoxide radicals ($\cdot\text{O}_2^-$). These ROS, together with the direct oxidation by photogenerated holes, mineralize organic pollutants into CO₂, H₂O and inorganic ions [125] (Fig. 5).

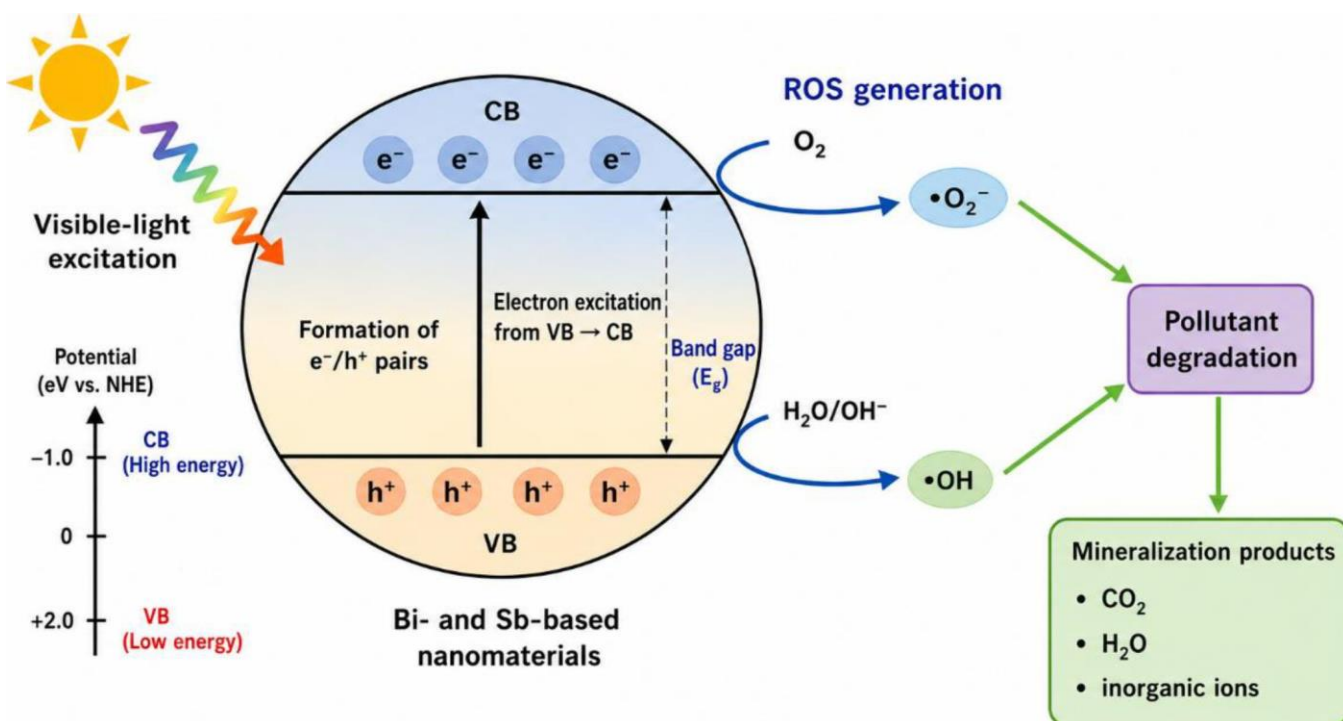


Fig. 5. Visible-light photocatalytic degradation mechanism in Bi- and Sb-based nanomaterials

The photocatalytic performance of Bi- and Sb-based materials is strongly influenced by the efficiency of charge separation and interfacial charge transfer. In conventional type-II heterojunctions, electrons migrate to the semiconductor with the lower CB potential, while holes transfer to the material with the higher VB potential, effectively suppressing electron-hole recombination. However, this spatial separation also lowers the redox potential since charge carriers accumulate at less energetic band positions. In contrast, Z-scheme heterojunctions selectively recombine low-energy electrons and holes while preserving highly reducing CB electrons and highly oxidising VB holes, thereby retaining strong redox capability. Similarly, S-scheme heterojunctions exploit built-in electric fields and band bending to promote directional charge migration and maintain charge carriers with high redox potentials. Consequently, Z-scheme and S-scheme architectures achieve superior charge separation, enhanced ROS generation and improved photocatalytic degradation compared with conventional type-II systems [80] (Fig. 6).

Photocatalytic activity is further enhanced through heteroatom doping, defect engineering and morphology control. Incorporation of suitable dopants can tailor the electronic band structure, extend visible-light absorption and facilitate interfacial charge transport. Surface oxygen vacancies act as electron trapping centers, prolonging charge-carrier lifetimes, suppressing electron-hole recombination and promoting the activation of adsorbed oxygen to generate ROS. In addition, exposed crystal facets and defect-rich surfaces provide abundant active sites for pollutant adsorption and interfacial redox reactions. The synergistic effects of optimized band structures, efficient charge separation, rapid interfacial charge transfer and enhanced ROS generation combined account for the outstanding photocatalytic performance of Bi- and Sb-based

nanomaterials in the degradation of a wide range of organic pollutants [124].

Surface interaction with pollutants: The adsorption performance of Bi- and Sb-based nanomaterials is governed by their surface chemistry, defect density and morphological characteristics. Surface oxygen vacancies (OVs), coordinatively unsaturated metal sites and abundant active surface sites enhance the chemisorption of pollutants by increasing adsorption affinity and facilitating interfacial charge transfer [126]. For organic contaminants, including cationic dyes and phenolic compounds, adsorption primarily occurs through coordination of electron-donating functional groups (*e.g.* O- or N-containing moieties) with exposed Bi or Sb surface atoms, together with electrostatic and π - π interactions where applicable. In contrast, heavy metal ions are predominantly adsorbed through inner-sphere complexation with surface hydroxyl groups and unsaturated metal coordination sites, resulting in stable surface complexes [127]. Furthermore, hierarchical nanostructures, such as nanosheets, nanoflowers and hollow architectures, provide high specific surface areas, abundant exposed crystal facets, and shortened diffusion pathways, thereby increasing the availability of adsorption sites while simultaneously promoting photocatalytic reactions.

Surface charge also plays a critical role in selective pollutant adsorption. Oxygen vacancies often impart localized negative charge and enhance electron density, promoting electrostatic attraction toward cationic pollutants such as methylene blue. Conversely, adsorption of anionic species is favoured at coordinatively unsaturated Bi³⁺ or Sb³⁺ surface centers that function as Lewis acid sites [128]. In metallic Bi-containing composites, the high electrical conductivity of Bi⁰ facilitates rapid electron transfer, thereby promoting reductive transformations of electron-accepting contaminants inclu-

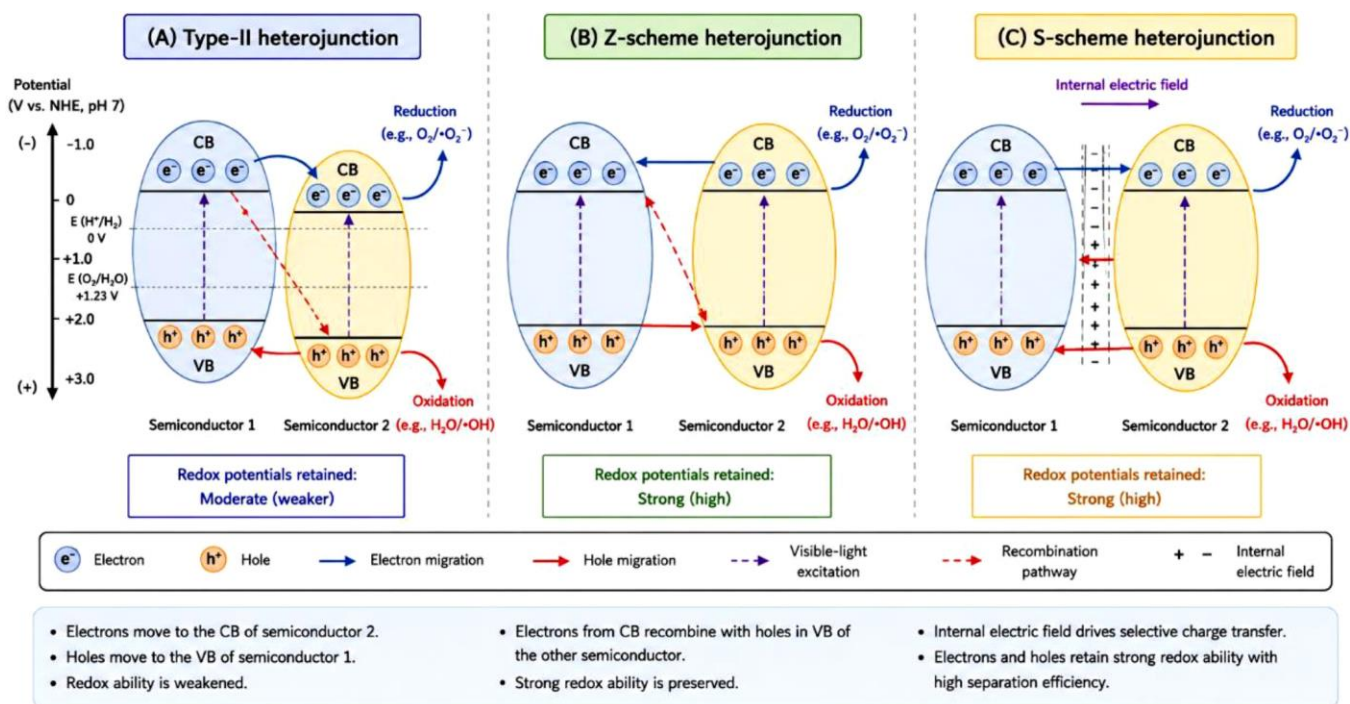


Fig. 6. Charge-transfer pathways and band alignment in type-II, Z-scheme and S-scheme photocatalytic heterojunctions under visible light

ding nitroaromatic compounds and Cr(VI), while suppressing charge-carrier recombination.

Surface functionalization with amino ($-\text{NH}_2$), hydroxyl ($-\text{OH}$), carboxyl ($-\text{COOH}$) or other polar functional groups further enhances adsorption by increasing the density of binding sites, improving surface hydrophilicity and lowering the activation energy for interfacial redox reactions [129]. Thus, the synergistic integration of defect engineering, morphology optimization, heterostructure design and surface functionalisation substantially improves pollutant adsorption, charge separation, ROS generation and photocatalytic degradation efficiency, making Bi- and Sb-based nanomaterials highly effective platforms for environmental remediation.

Electron-hole pair dynamics: The efficient separation, migration and utilization of photogenerated electron-hole pairs are among the most critical factors governing the photocatalytic quantum efficiency of Bi- and Sb-based nanomaterials. In layered BiOX photocatalysts, the asymmetric $[\text{Bi}_2\text{O}_2]^{2+}$ slabs generate intrinsic internal electric fields that promote directional charge migration and suppress electron-hole recombination, thereby enhancing photocatalytic performance [130]. Likewise, the polar crystal structure of Bi_2WO_6 facilitates efficient spatial separation of photogenerated charge carriers, resulting in improved photocatalytic activity.

Oxygen vacancies (OVs) play a pivotal role in charge-carrier dynamics by acting as electron-trapping centres that temporarily capture photogenerated electrons. This process prolongs carrier lifetimes, suppresses charge recombination and increases the availability of electrons for interfacial redox reactions [130]. The trapped electrons readily reduce adsorbed oxygen molecules to produce reactive oxygen species (ROS), particularly superoxide radicals ($\cdot\text{O}_2^-$), which are key oxidising intermediates in photocatalytic degradation. Another effective strategy for enhancing photocatalytic efficiency is heteroatom doping. For example, Sb doping in BiVO_4 modifies the electronic band structure by introducing intermediate energy levels and defect states within the band gap, thereby facilitating charge transfer, improving carrier mobility and minimising recombination losses [131].

The construction of semiconductor heterojunctions with materials such as TiO_2 , $g\text{-C}_3\text{N}_4$ and Sb_2S_3 further improves charge-separation efficiency. In conventional Type-II heterojunctions, photogenerated electrons and holes migrate to different semiconductor components according to their band alignments, effectively suppressing recombination. In contrast, Z-scheme and S-scheme heterojunctions preserve highly energetic electrons and holes with strong reduction and oxidation potentials, respectively, thereby maintaining superior redox capability while enhancing charge separation [80]. Accordingly, these architectures promote the generation of abundant ROS and significantly accelerate photocatalytic degradation reactions.

In addition, plasmonic Bi nanoparticles exhibit localized surface plasmon resonance (LSPR), enabling enhanced visible-light harvesting and the generation of energetic hot electrons that can be injected into adjacent semiconductor phases. This plasmon-induced charge transfer substantially improves photocatalytic efficiency by accelerating interfacial electron transport and broadening the photoresponse. Advanced characterisation techniques, including time-resolved photoluminescence

(TRPL) and transient absorption spectroscopy (TAS), have demonstrated that optimized Bi- and Sb-based heterostructures can prolong charge-carrier lifetimes from the picosecond to microsecond timescale, providing compelling evidence for enhanced charge separation and superior photocatalytic performance [131].

Structure-activity correlation: The structure-activity relationships indicate that the morphology, crystal facets, particle size (defect density), and elemental doping of Bi- and Sb-based nanomaterials will have a major influence on their photocatalytic properties (Fig. 7). For instance, BiOCl nanosheets predominantly exposing the (001) crystal facet exhibits superior photocatalytic activity owing to their high density of oxygen vacancies and the strong internal electric fields that facilitate efficient charge separation [73]. Similarly, ultrathin 2D Bi_2WO_6 nanosheets provide shorter charge-carrier diffusion pathways and enhanced visible-light absorption, thereby improving the photocatalytic efficiency.

Hierarchical three-dimensional architectures, including nanoflowers and microspheres assembled from nanoscale building blocks, offer large specific surface areas, enhanced light scattering and abundant active sites, jointly promoting pollutant adsorption and photocatalytic reactions. Particle size optimisation is equally important, as it balances surface reactivity, light-harvesting capability and charge-transfer efficiency. Nanoparticles with sizes in the range of approximately 20-50 nm often exhibit optimal photocatalytic performance by maximising surface-active sites while minimising charge-carrier recombination [132].

Defect engineering and elemental doping are highly effective strategies for enhancing photocatalytic activity. Oxygen vacancies serve as electron-trapping centers that prolong charge carrier lifetimes, suppress electron-hole recombination, and promote the generation of ROS, thereby accelerating photocatalytic oxidation processes [133]. Likewise, Sb doping in BiVO_4 narrows the band gap, optimizes band-edge positions, and enhances visible-light absorption, resulting in improved charge transport and higher photocatalytic efficiency. More broadly, controlled defect formation and heteroatom incorporation enable precise tuning of the electronic structure, carrier mobility and catalytic activity of Bi- and Sb-based photocatalysts.

Furthermore, quantitative structure-property relationship (QSPR) analysis has emerged as a powerful framework for correlating the physico-chemical characteristics of photocatalysts with their functional performance. Key descriptors, including band-gap energy, specific surface area, oxygen-vacancy density, average crystallite size and charge-carrier lifetime, can be quantitatively correlated with photocatalytic degradation rates and ROS generation. In general, higher oxygen vacancy densities and longer carrier lifetimes promote more efficient charge separation and faster degradation kinetics, whereas optimized band-edge positions and larger surface areas enhance visible-light utilization and facilitate pollutant adsorption. Consequently, QSPR-guided design provides a rational, data-driven strategy for developing highly efficient Bi- and Sb-based photocatalysts with optimized structural, electronic and photocatalytic properties.

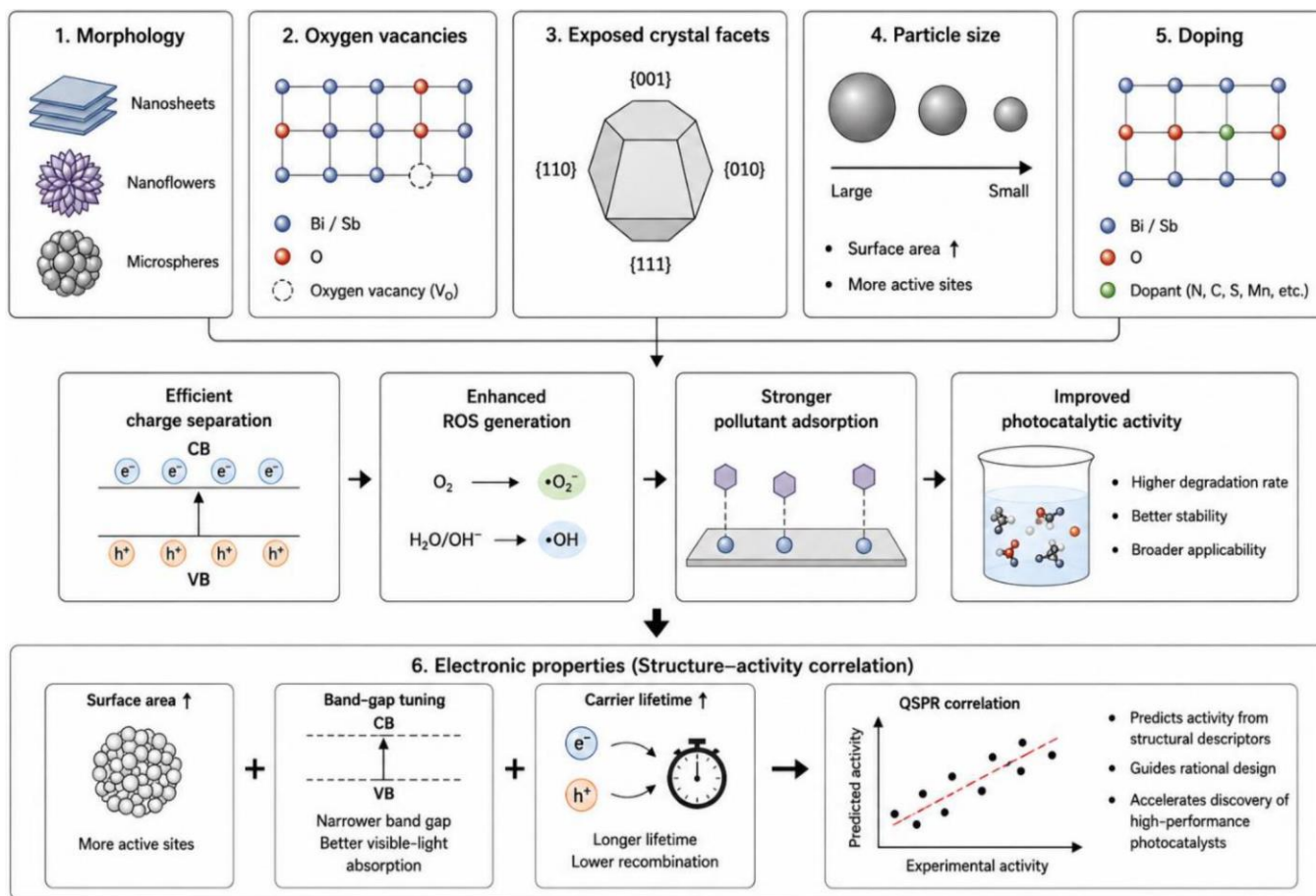


Fig. 7. Structure–activity correlation in Bi- and Sb-based photocatalysts influencing charge separation and photocatalytic activity

Challenges and limitations: Bi- and Sb-based nanomaterials have emerged as promising photocatalysts for environmental remediation owing to their excellent visible-light responsiveness and tunable electronic properties. Despite their considerable potential, several challenges continue to hinder their large-scale commercial implementation. Key limitations include photocorrosion, catalyst deactivation, metal-ion leaching, nanoparticle agglomeration, difficulties in scalable synthesis, concerns regarding long-term toxicity and environmental safety, and the lack of efficient industrial-scale photoreactor designs. Addressing these challenges is essential for translating laboratory-scale advances into economically viable and sustainable photocatalytic technologies for practical environmental applications [28].

Stability, photocorrosion and agglomeration issues:

The photocatalytic activity of Bi and Sb based nanomaterials, like Bi_2O_3 , is high, but their initial photocatalytic activity will often decrease over time when exposed to intense light [42]. The photocatalytic activity of Bi_2O_3 can also result in dissolved Bi^{3+} being formed and catalytic activity decreasing due to self-photoreduction or self-photooxidation. Also, Bi in the metallic form has shown the ability to oxidize rapidly in an aqueous environment. This oxidised layer of Bi will create an insulating barrier, reduce the conductivity of these materials and inhibiting the movement of electrons [100]. In addition, the photocatalytic materials BiOX will lose halides at the elevated reaction temperatures.

Aggregation or agglomeration, of nanoparticles is also a major drawback of photocatalytic systems; nanoparticle aggregation results in reduced available active surface area and number of catalyst sites for photocatalytic applications in modern wastewater treatment systems operating at high ionic strengths. In addition, deactivation of the photocatalyst, from deposition of foreign material on the photocatalyst surface, binding of intermediates to catalyst surfaces (surface-bound intermediate products) and multiple photocatalytic activity (or turnover) cycles, decreases the long-term stability and recyclability of photocatalytic devices. Several surface modification approaches have been investigated to help improve the stability of dispersed nanoparticle systems from photocorrosion or free radical attacks, including coating photocatalysts with SiO_2 , polymer and some types of graphene derivatives, as well as immobilizing photocatalysts on solid support materials; however, these approaches increase the complexity of photocatalytic systems and the costs associated with synthesising and operating photocatalytic devices [134]. Recent work investigating the charge separation efficiency and photocorrosion resistance of S-scheme heterojunction photocatalysts and oxygen-vacancy engineered Bi-based systems has shown a substantial improvement in photocorrosion resistance as well as the charge separation efficiency [135].

Scalability and industrial reactor challenges: Green synthesis offers an environmentally benign approach for

producing Bi- and Sb-based nanoparticles by utilizing plant extracts, microorganisms and biomolecules as reducing and stabilising agents, thereby minimizing the use of hazardous chemicals and reducing the environmental footprint of nanomaterial production [134]. However, the commercial-scale implementation of green synthesis remains challenging since the composition of naturally derived phytochemicals varies with plant species, growth conditions and extraction methods, resulting in inconsistencies in nanoparticle morphology, crystallinity, particle size and photocatalytic performance. Furthermore, biologically synthesised nanoparticles often exhibit relatively low production yields, slower reaction kinetics and residual organic capping agents that complicate purification, reduce catalyst stability, and may partially block catalytically active surface sites [136].

Conventional hydrothermal and chemical reduction methods provide superior control over particle size, morphology, crystallinity and composition, enabling the synthesis of highly reproducible photocatalysts. Nevertheless, these approaches typically require elevated temperatures and pressures, high energy consumption and the use of hazardous organic solvents or chemical reducing agents, limiting their environmental sustainability and increasing production costs [137]. Therefore, translating laboratory-scale synthesis into economically viable industrial production requires advances in scalable fabrication processes, catalyst immobilization strategies, continuous-flow synthesis and efficient catalyst recovery and recycling.

Beyond material synthesis, photoreactor engineering remains one of the principal barriers to the large-scale deployment of photocatalytic technologies. Industrial-scale systems frequently suffer from limited light penetration, inefficient photon utilisation, mass-transfer limitations, catalyst sedimentation, membrane fouling and difficulties in maintaining uniform catalyst dispersion, all of which reduce photocatalytic efficiency. Although recent developments in continuous-flow annular photoreactors and photocatalytic membrane reactors have demonstrated improved scalability and enhanced wastewater treatment performance, further optimization is required to improve long-term operational stability, energy efficiency and economic feasibility before these technologies can be widely commercialized [138,139].

Toxicity, metal-ion leaching and environmental concerns: Bi-based nanomaterials are generally regarded as more biocompatible and less toxic than many conventional heavy-metal nanomaterials, making them attractive candidates for environmental and biomedical applications. Nevertheless, excessive exposure to Bi-based nanomaterials may induce cytotoxic effects through the generation of ROS, oxidative stress, and the release of Bi ions under specific environmental conditions [140]. Recent studies have also shown that Bi₂S₃ nanomaterials can accumulate in aquatic organisms at elevated concentrations, disrupting metabolic processes and raising concerns regarding their long-term ecological impacts [141].

Metal-ion leaching during photocatalytic operation represents another important environmental challenge. Under acidic or strongly oxidative conditions, the dissolution of Bi³⁺ and Sb³⁺ ions from photocatalysts may contaminate treated water and increase ecological risks. Although Bi-based nanomaterials

generally exhibit lower toxicity than their Sb-based counterparts, antimony-containing nanomaterials require more attention due to the inherently higher toxicity of Sb species. In particular, Sb³⁺ ions promote oxidative stress, induce mitochondrial dysfunction, DNA damage and apoptosis, and have been reported to produce dose-dependent toxic effects in algae, aquatic organisms and amphibians, highlighting their potential ecological hazards [142]. Consequently, strategies that minimise metal-ion leaching, such as surface passivation, protective coatings and catalyst immobilization, are essential for ensuring the long-term environmental safety of Sb-containing photocatalysts.

Despite growing interest in Bi- and Sb-based nanomaterials, comprehensive information regarding their long-term environmental fate and biological safety remains limited. Critical knowledge gaps persist concerning chronic toxicity, bioaccumulation, biodegradation, transformation pathways and long-term environmental persistence. Furthermore, standardised protocols and regulatory frameworks for evaluating the environmental and human health risks of these nanomaterials are still under development, limiting consistent risk assessment and safe implementation [143]. Therefore, comprehensive life-cycle assessments, quantitative environmental risk analyses and standardized toxicological evaluations are essential before the large-scale deployment of Bi- and Sb-based photocatalysts. Recent studies on Bi(III) and Sb(III) complexes further emphasise the need for rigorous biological safety assessments to ensure the responsible use of these nanomaterials in both environmental remediation and biomedical applications [144].

Commercialisation challenges: At present, photocatalytic technologies based on Bi- and Sb-containing nanomaterials remain at an early stage of technological development, with most systems evaluated only at the laboratory scale, corresponding to approximately Technology Readiness Levels (TRLs) 2-4. Although these photocatalysts have demonstrated excellent visible-light-driven activity and pollutant degradation efficiencies under controlled laboratory conditions, only a limited number of pilot-scale studies have been reported, and industrial-scale implementation remains largely unexplored. The principal barriers to commercialization include insufficient long-term catalyst stability, photocorrosion-induced deactivation, inefficient catalyst recovery and recycling, and the absence of optimized photoreactor designs capable of operating under realistic wastewater treatment conditions [21,138].

Economic considerations further constrain large-scale deployment. The relatively high cost of precursor materials, energy-intensive synthesis procedures, complex purification processes, and the requirement for specialized photoreactor configurations contribute substantially to the capital and operating costs of photocatalytic systems [137,145]. In addition, the limited solar-to-chemical conversion efficiency of current photocatalysts often necessitates artificial light sources to achieve practical treatment rates, resulting in increased electricity consumption and higher operational expenses. Although catalyst recovery techniques including membrane filtration, catalyst immobilisation, magnetic separation (where applicable) and centrifugation, can improve catalyst reusability,

these additional processing steps increase system complexity, energy demand and maintenance costs, thereby reducing the economic and environmental sustainability of the technology [146].

Beyond technical and economic challenges, regulatory and standardisation issues continue to impede commercialisation. The lack of standardized testing protocols for photocatalytic performance, catalyst durability, nanomaterial release and environmental safety hinders meaningful comparisons between studies and complicates technology validation. Furthermore, the absence of comprehensive regulatory frameworks governing the manufacture, application, recovery and disposal of nanomaterial-based photocatalysts presents additional barriers to industrial adoption, particularly for wastewater treatment applications [143]. So, future commercialization will require not only advances in photocatalyst design and reactor engineering but also the development of standardized evaluation protocols, life-cycle assessment methodologies, techno-economic analyses and clear regulatory guidelines to ensure the safe, cost-effective and sustainable deployment of Bi- and Sb-based photocatalytic technologies.

Critical analysis and future perspectives: Recent bibliometric analyses highlight the rapidly expanding research interest in Bi- and Sb-based photocatalytic nanomaterials for environmental remediation, driven by their excellent visible-light responsiveness, tunable electronic structures, and comparatively favourable environmental compatibility [7,119]. Current research is increasingly directed toward heterojunction engineering, oxygen-vacancy modulation, plasmonic enhancement and integration with carbon-based materials to maximise solar-light harvesting, accelerate charge separation and improve photocatalytic efficiency. Representative systems, including BiVO₄/g-C₃N₄, BiOX/TiO₂ and Sb-graphene heterostructures, have demonstrated remarkable performance for the degradation of dyes, pharmaceuticals, antibiotics and other emerging contaminants under visible-light or solar irradiation [7].

Despite these advances, several scientific and technological challenges continue to impede practical implementation. Although photocatalysts such as BiVO₄, BiOX and Sb₂S₃ exhibit excellent visible-light absorption and catalytic activity, their performance is frequently constrained by rapid electron-hole recombination, photocorrosion, catalyst deactivation, metal-ion leaching, and limited long-term operational stability [77-79]. Furthermore, the majority of photocatalytic investigations are performed under idealized laboratory conditions using model pollutants, which do not adequately represent the complexity of real wastewater matrices containing diverse organic contaminants, inorganic ions and natural organic matter [108]. Consequently, the translation of laboratory-scale performance to practical wastewater treatment remains a significant challenge.

Among the numerous material-engineering strategies explored, heterojunction engineering, particularly Z-scheme and S-scheme architectures has emerged as one of the most effective approaches for simultaneously promoting charge separation and preserving strong redox potentials. Compared with conventional Type-II heterojunctions, these advanced architectures generally exhibit superior ROS generation, en-

anced mineralisation efficiency and improved photocatalytic stability [80]. Nevertheless, a deeper understanding of interfacial charge-transfer pathways, band alignment, defect chemistry and surface reaction mechanisms remains essential for the rational design of next-generation photocatalysts with predictable and reproducible performance [80,124].

Significant advances in characterization techniques have substantially improved the understanding of SARs in Bi- and Sb-based photocatalysts. Conventional techniques, *e.g.* XRD, XPS, FTIR, UV-Vis DRS, PL spectroscopy, electron microscopy and electrochemical analyses, have provided valuable insights into crystal structure, electronic properties, defect states and charge-transfer behaviour [28,56-62]. More recently, operando and *in situ* characterization methods, such as *in situ* XPS, Raman spectroscopy, transient absorption spectroscopy (TAS) and time-resolved photoluminescence (TRPL), have enabled direct observation of reaction intermediates and charge carrier dynamics under realistic operating conditions, offering unprecedented opportunities to elucidate photocatalytic mechanisms and guide catalyst optimization.

From a commercialization perspective, scalable synthesis, reproducibility, catalyst durability and environmental safety remain major concerns. Hydrothermal synthesis offers excellent control over crystallinity and morphology but is associated with high energy consumption, batch processing, and limited scalability. On the other hand, green synthesis provides an environmentally sustainable alternative but often suffers from batch-to-batch variability, inconsistent product quality and lower reproducibility owing to the variable composition of biological precursors [50-54]. The microwave-assisted synthesis, electrochemical fabrication, continuous-flow processing and other scalable manufacturing techniques are attracting increasing attention as promising routes for the industrial photocatalyst production [28,119]. In parallel, the potential toxicity, environmental persistence and metal-ion leaching associated with Sb-containing nanomaterials necessitate comprehensive life-cycle assessments, standardized ecotoxicological evaluations and rigorous environmental risk analyses before large-scale deployment [41,121].

Future research should prioritise the development of highly stable, recyclable and environmentally benign photocatalysts through integrated strategies encompassing defect engineering, heterostructure design, cocatalyst incorporation, surface passivation and sustainable synthesis methods. In addition, the integration of artificial intelligence (AI), machine learning (ML), density functional theory (DFT) and high-throughput computational screening is expected to accelerate materials discovery by enabling predictive optimisation of band structures, defect configurations, adsorption energetics and charge-transfer pathways at the atomic scale [119]. These computational approaches, combined with advanced experimental characterisation, will facilitate the rational design of high-performance photocatalysts with tailored physico-chemical properties.

Equally important is the transition from laboratory investigations to practical implementation through pilot-scale demonstrations, long-term stability assessments, techno-economic analyses and validation under real wastewater treatment conditions. Establishing standardised testing protocols and regula-

tory frameworks will further facilitate meaningful performance comparisons and accelerate technology transfer from academic research to industrial applications. Finally, integrating Bi- and Sb-based photocatalytic systems with complementary sustainable technologies including hydrogen evolution, CO₂ photo-reduction, nutrient recovery and circular-economy strategies, offers significant opportunities to enhance both environmental and economic sustainability. Continued progress in materials engineering, computational materials design, scalable manufacturing, and reactor engineering is expected to position Bi- and Sb-based nanomaterials among the most promising next-generation photocatalysts for sustainable water purification, environmental remediation, solar-energy conversion and integrated resource-recovery applications [119].

Conclusions

Bismuth (Bi)- and antimony (Sb)-based nanomaterials have attracted considerable attention as visible-light-responsive photocatalysts due to their tunable electronic structures, favorable redox potentials and compatibility with advanced heterojunction architectures. Precise control over morphology, crystal facets, oxygen vacancies, elemental doping and surface modification has markedly improved light absorption, charge separation, and photocatalytic efficiency. Z- and S-schemes heterojunctions have shown particular promise by maintaining strong redox ability while suppressing electron-hole recombination, enabling efficient degradation of dyes, pharmaceuticals, pesticides, antibiotics and toxic metal ions. However, commercial implementation remains challenging. Photocorrosion, catalyst deactivation, nanoparticle agglomeration, metal-ion leaching and limited catalyst recyclability reduce long-term performance. Scalable synthesis, reproducibility and stable operation under realistic wastewater conditions have yet to be fully established. Uncertainties related to environmental fate, chronic toxicity, bioaccumulation and life-cycle impacts, particularly for Sb-based materials, require systematic investigation before widespread application can be considered.

Future progress depends on scalable green synthesis, durable heterostructure design, effective catalyst immobilisation and energy-efficient photoreactor development. Advanced computational tools, artificial intelligence, machine learning, density functional theory and operando characterization will accelerate materials optimization by revealing structure–property relationships and charge-transfer mechanisms. Standardised testing protocols, life-cycle assessment, techno-economic analysis and regulatory frameworks are equally important for ensuring reliable performance and environmental safety. Hence, continuous progress in materials design, reactor engineering and safety assessment will determine their successful transition from laboratory research to industrial application.

CONFLICT OF INTEREST

The authors declare that there is no conflict of interests regarding the publication of this article.

DECLARATION OF AI-ASSISTED TECHNOLOGIES

During the preparation of this manuscript, the authors used an AI-assisted tool(s) to improve the language. The authors reviewed and edited the content and take full responsibility for the published work.

REFERENCES

- Nishu and S. Kumar, *Hybrid Adv.*, **3**, 100044 (2023); <https://doi.org/10.1016/j.hybadv.2023.100044>.
- A.R. Dhanapal, M. Thiruvengadam, J. Vairavanathan, B. Venkidasamy, M. Easwaran and M. Ghorbanpour, *ACS Omega*, **9**, 13522 (2024); <https://doi.org/10.1021/acsomega.3c09776>.
- R. Abbasi, G. Shineh, M. Mobaraki, S. Doughty and L. Tayebi, *J. Nanopart. Res.*, **25**, 43 (2023); <https://doi.org/10.1007/s11051-023-05690-w>.
- M. Kholopo and P.C. Rathebe, *Sustain. Environ.*, **11**, 2558248 (2025); <https://doi.org/10.1080/27658511.2025.2558248>.
- O.P. Onotu, H.S. Samuel, D.A. Undie, O.O. Akinpelu, F.A. Ibekwe and E.E. Etim, *Discov. Nano*, **20**, 191 (2025); <https://doi.org/10.1186/s11671-025-04341-4>.
- S. Velusamy, A. Roy, S. Sundaram and T. Kumar Mallick, *Chem. Rec.*, **21**, 1570 (2021); <https://doi.org/10.1002/tcr.202000153>.
- T.L. Wakjira, A.B. Gemta, G.B. Kassahun, D.M. Andoshe and K. Tadele, *ACS Omega*, **9**, 8709 (2024); <https://doi.org/10.1021/acsomega.3c08939>.
- M. Sachs, R.S. Sprick, D. Pearce, S.A.J. Hillman, A. Monti, A.A.Y. Guilbert, N.J. Brownbill, S. Dimitrov, X. Shi, F. Blanc, M.A. Zwijnenburg, J. Nelson, J.R. Durrant and A.I. Cooper, *Nat. Commun.*, **9**, 4968 (2018); <https://doi.org/10.1038/s41467-018-07420-6>.
- Š. Kment, A. Bakandritsos, I. Tantis, H. Kmentová, Y. Zuo, O. Henrotte, A. Naldoni, M. Otyepka, R.S. Varma and R. Zbořil, *Chem. Rev.*, **124**, 11767 (2024); <https://doi.org/10.1021/acs.chemrev.4c00155>.
- K. Chen, W. Dong, Y. Huang, F. Wang, J.L. Zhou and W. Li, *J. Environ. Chem. Eng.*, **13**, 117529 (2025); <https://doi.org/10.1016/j.jece.2025.117529>.
- T. Ishaq, Z. Ehsan, A. Qayyum, Y. Abbas, A. Irfan, S.A. Al-Hussain, M.A. Irshad and M.E.A. Zaki, *Catalysts*, **14**, 674 (2024); <https://doi.org/10.3390/catal14100674>.
- K.M. Mohamed, J.J. Benitto, J.J. Vijaya and M. Bououdina, *Crystals*, **13**, 329 (2023); <https://doi.org/10.3390/cryst13020329>.
- D. Xu, H. Cai, D. Li, F. Chen, S. Han, X. Chen, Z. Li, Z. He, Z. Chen, J. He, W. Huang, X. Tang, Y. Wen and Y. Feng, *Inorganics*, **13**, 319 (2025); <https://doi.org/10.3390/inorganics13100319>.
- M. Bouziani, A. Bouziani, A. Hsini, C.L. Bianchi, E. Falletta, G. Cerrato, A. Giordana, G. Çelik and R. Hausler, *J. Hazard. Mater. Adv.*, **21**, 101064 (2026); <https://doi.org/10.1016/j.hazadv.2026.101064>.
- J.O. Adeyemi and D.C. Onwudiwe, *Molecules*, **25**, 305 (2020); <https://doi.org/10.3390/molecules25020305>.
- O. Planas, V. Peciukenas and J. Cornella, *J. Am. Chem. Soc.*, **142**, 11382 (2020); <https://doi.org/10.1021/jacs.0c05343>.
- Y. Jiang, Y. Guo, Y. Zhou, S. Deng, L. Hou, Y. Niu and T. Jiao, *ACS Omega*, **5**, 14805 (2020); <https://doi.org/10.1021/acsomega.0c01859>.
- X. Lu, L. Wang, Z. Li, Z. Wang, Y. Gan and R. Hailili, *ACS Sustain. Chem. & Eng.*, **12**, 11444 (2024); <https://doi.org/10.1021/acssuschemeng.4c03627>.
- J. Ahmadi, V.B.K. Yaah, S.B. de Oliveira and S. Ojala, *J. Clean. Prod.*, **523**, 146456 (2025); <https://doi.org/10.1016/j.jclepro.2025.146456>.
- D. Raabe, *Chem. Rev.*, **123**, 2436 (2023); <https://doi.org/10.1021/acs.chemrev.2c00799>.
- B.O. Orimolade, M.G. Peleyeju and T.L. Yusuf, *J. Environ. Manage.*, **397**, 128319 (2026); <https://doi.org/10.1016/j.jenvman.2025.128319>.

22. A.E. Hughes, N. Haque, S.A. Northey and S. Giddey, *Resources*, **10**, 93 (2021); <https://doi.org/10.3390/resources10090093>
23. S. Sarwar, S. Ali, S.R. Khan, S. Jamil, S. Farooq, T. Jafar, M.J. Latif and H. Shehroz, *Environ. Technol. Rev.*, **13**, 544 (2024); <https://doi.org/10.1080/21622515.2024.2380830>
24. S. Kumar, M. Premkumar, J. Giri, S.M.M. Hasnain, R. Zairov, J. Wu and Z. Huang, *RSC Adv.*, **14**, 39523 (2024); <https://doi.org/10.1039/D4RA05637J>
25. J. Biemolt, P. Jungbacker, T. van Teijlingen, N. Yan and G. Rothenberg, *Materials*, **13**, 425 (2020); <https://doi.org/10.3390/ma13020425>
26. J. Di, J. Xia, M. Ji, H. Xu, H. Xu, S. Zhang and L. Li, *Chem. Soc. Rev.*, **46**, 731 (2017); <https://doi.org/10.1039/C6CS00599A>
27. J. Low, B. Dai, T. Tong, C. Jiang and J. Yu, *Adv. Mater.*, **31**, 1802981 (2019); <https://doi.org/10.1002/adma.201802981>
28. R.M. Clark, J.C. Kotsakidis, B. Weber, K.J. Berean, B.J. Carey, M.R. Field, H. Khan, J.Z. Ou, T. Ahmed, C.J. Harrison, I.S. Cole, K. Latham, K. Kalantar-zadeh and T. Daeneke, *Chem. Mater.*, **28**, 8942 (2016); <https://doi.org/10.1021/acs.chemmater.6b03478>
29. S. Adhikari, S. Mandal and D.H. Kim, *Small*, **19**, 2206003 (2023); <https://doi.org/10.1002/smll.202206003>
30. G.V. Tikhonowski, A.A. Popov, I. Zelepukin, E. Popova-Kuznetsova, Y.I. Dombrowska, S.M. Deev, I.N. Zavestovskaya, S.M. Klimentov, P.N. Prasad and A.V. Kabashin, **11990**, 22 (2022); <https://doi.org/10.1117/12.2615386>
31. I. Khan, K. Saeed and I. Khan, *Arab. J. Chem.*, **12**, 908 (2019); <https://doi.org/10.1016/j.arabjc.2017.05.011>
32. Y. Zhang and J. Di, Layered Bismuth-Based Photocatalysts 1: BiOX (X = Cl, Br, I), In: Layered Materials in Photocatalysis: Environmental Purification and Energy Conversion, Wiley, Chap. 4 (2025).
33. M. Li, T. Wang, Y. Zhao and X. Chen, *Appl. Mater. Today*, **44**, 102791 (2025); <https://doi.org/10.1016/j.apmt.2025.102791>
34. A. Shongalova, M. Petrova and D. Ivanov, *Processes*, **13**, 3560 (2025); <https://doi.org/10.3390/pr13113560>
35. V. Calzia, A. Fiore, D. Barreca and E. Tondello, *J. Phys. Chem. C Nanomater. Interfaces*, **117**, 21923 (2013); <https://doi.org/10.1021/jp405740b>
36. S. Mahmud, N. Zhang and K.V. Nedunuri Kumar, *R. Soc. Open Sci.*, **12**, 241506 (2025); <https://doi.org/10.1098/rsos.241506>
37. N. Baig, I. Kammakakam, W. Falath and I. Kammakakam, *Mater. Adv.*, **2**, 1821 (2021); <https://doi.org/10.1039/D0MA00807A>
38. V. Dutta, A. Chauhan, R. Verma, C. Gopalkrishnan and V.-H. Nguyen, *Beilstein J. Nanotechnol.*, **13**, 1316 (2022); <https://doi.org/10.3762/bjnano.13.109>
39. A. Shongalova, A. Kemelbekova, A. Umirzakov, I. Tashmukhanbetova and E. Dmitriyeva, *Processes*, **13**, 3560 (2025); <https://doi.org/10.3390/pr13113560>
40. T. Khandaker, M.A.A.M. Anik, A. Nandi, T. Islam, M.M. Islam, M.K. Hasan, P.K. Dhar, M.A. Latif and M.S. Hossain, *Catal. Sci. Technol.*, **15**, 1357 (2025); <https://doi.org/10.1039/D4CY01171F>
41. Â. Gonçalves, M. Matias, J.A.R. Salvador and S. Silvestre, *Int. J. Mol. Sci.*, **25**, 1600 (2024); <https://doi.org/10.3390/ijms25031600>
42. X. Yang et al., *Catalysts*, **15**, (2025); <https://doi.org/10.3390/CATAL15080714/S1>
43. J. Thomas, V. Kumar, N. Sharma, N. John, M. Umesh, L.K.D. Huligowda, K. Kaur and D. Utreja, *Med. Drug Discov.*, **25**, 100204 (2025); <https://doi.org/10.1016/j.medidd.2025.100204>
44. X. Duan, Y. Yang, T. Zhang, B. Zhu, G. Wei and H. Li, *Heliyon*, **10**, e25515 (2024); <https://doi.org/10.1016/j.heliyon.2024.e25515>
45. M. Mahiuddin and B. Ochiai, *ACS Omega*, **7**, 35626 (2022); <https://doi.org/10.1021/acsomega.2c03416>
46. F. Zaera, *ChemSusChem*, **6**, 1797 (2013); <https://doi.org/10.1002/cssc.201300398>
47. S.T. Shah, I.P. Sari, D.H.Y. Yanto, Z.Z. Chowdhury, M.N. Bashir, I.A. Badruddin, M. Hussien and J.S. Lee, *Green Chem. Lett. Rev.*, **18**, 2448171 (2025); <https://doi.org/10.1080/17518253.2024.2448171>
48. E. AlShamaleh, B. Lahlouh, A.N. AL-Masri and I.S. Moosa, *Coatings*, **15**, 1118 (2025); <https://doi.org/10.3390/coatings15101118>
49. D.A. Peixoto, S.C. Silva, P.H.S. Borges, R.C. Lima and E. Nossol, *J. Mater. Sci.*, **58**, 2993 (2023); <https://doi.org/10.1007/s10853-023-08190-3>
50. J. Plotka-Wasyłka, M. Rutkowska, K. Owczarek, M. Tobiszewski and J. Namieśnik, *Trends Analyt. Chem.*, **91**, 12 (2017); <https://doi.org/10.1016/j.trac.2017.03.006>
51. M.D.K.M. Gunasena, G.D.C.P. Galpaya, C.J. Abeygunawardena, D.K.A. Induranga, H.V.V. Priyadarshana, S.S. Millavithanachchi, P.K.G.S.S. Bandara and K.R. Koswattage, *Nanomaterials*, **15**, 528 (2025); <https://doi.org/10.3390/nano15070528>
52. M. Mahiuddin and B. Ochiai, *RSC Adv.*, **11**, 26683 (2021); <https://doi.org/10.1039/D1RA03560F>
53. S. Singaravelu, F. Motsoene, H. Abrahamse and S.S. Dhillip Kumar, *Front. Bioeng. Biotechnol.*, **13**, 1637589 (2025); <https://doi.org/10.3389/fbioe.2025.1637589>
54. M.B. Gawande, S.N. Shelke, R. Zboril and R.S. Varma, *Acc. Chem. Res.*, **47**, 1338 (2014); <https://doi.org/10.1021/ar400309b>
55. B. Zhang, X. Ye, W. Hou, Y. Zhao and Y. Xie, *J. Phys. Chem. B*, **110**, 8978 (2006); <https://doi.org/10.1021/jp060769j>
56. F. Zhang, X. Wang, H. Liu, C. Liu, Y. Wan, Y. Long and Z. Cai, *Appl. Sci.*, **9**, 2489 (2019); <https://doi.org/10.3390/app9122489>
57. J.Z. Hassan, A. Raza, U. Qumar and G. Li, *Sustain. Mater. Technol.*, **33**, e00478 (2022); <https://doi.org/10.1016/j.susmat.2022.e00478>
58. J. Tian, J. Li, Y. Guo, Z. Liu, B. Liu and J. Li, *Adv. Powder Mater.*, **3**, 100201 (2024); <https://doi.org/10.1016/j.apmate.2024.100201>
59. X. Li, J. Yu, J. Low, Y. Fang, J. Xiao and X. Chen, *J. Mater. Chem. A Mater. Energy Sustain.*, **3**, 2485 (2015); <https://doi.org/10.1039/C4TA04461D>
60. M. Sittishoktram, P. Yaemsanguansak, R. Tuayjaroen, P. Asanithi and T. Jutarosaga, *Mater. Sci. Semicond. Process.*, **108**, 104886 (2020); <https://doi.org/10.1016/j.mssp.2019.104886>
61. P. Karthik, R. Vinoth, S. Ganesh Babu, M. Wen, T. Kamegawa, H. Yamashita and B. Neppolian, *RSC Adv.*, **5**, 39752 (2015); <https://doi.org/10.1039/c5ra03831f>
62. Y. Liang, J. Manioudakis, J.R. Macairan, M.S. Askari, P. Forgione and R. Naccache, *ACS Omega*, **4**, 14955 (2019); <https://doi.org/10.1021/acsomega.9b01736>
63. M.L. Personick, *J. Phys. Chem. C Nanomater. Interfaces*, **128**, 8131 (2024); <https://doi.org/10.1021/acs.jpcc.4c00851>
64. A. Quintanilla, U. Valvo, E.M. Lafont, M.T. Kelder, M. Kreutzer and F. Kapteijn, *Chem. Mater.*, **22**, 1656 (2010); <https://doi.org/10.1021/cm903712y>
65. S.H. Feng and G.H. Li, in eds.: R. Xu, Y. Xu and H. Xu, Hydrothermal and Solvothermal Syntheses, In: Modern Inorganic Synthetic Chemistry, Eds. Amsterdam, The Netherlands: Elsevier, pp. 73-104 (2017).
66. R. He, D. Xu, B. Cheng, J. Yu and W. Ho, *Nanoscale Horiz.*, **3**, 464 (2018); <https://doi.org/10.1039/C8NH00062J>
67. T.Q. Tazim, M. Kawsar, M. Sahadat Hossain, N.M. Bahadur and S. Ahmed, *Next Nanotechnol.*, **7**, 100167 (2025); <https://doi.org/10.1016/j.nxnano.2025.100167>
68. A.S. Dousari, M. Shakibaie, M. Adeli-Sardou and H. Forootanfar, *Biol. Trace Elem. Res.*, **203**, 3949 (2024); <https://doi.org/10.1007/s12011-024-04437-5>
69. V. Thirumal, R. Yuvakkumar, P. Senthil Kumar, B. Saravanakumar, G. Ravi, M. Shobana and D. Velauthapillai, *Fuel*, **325**, 124908 (2022); <https://doi.org/10.1016/j.fuel.2022.124908>
70. L. Wu, C.H. Tan and X. Ye, *ACS Org. Inorg. Au*, **5**, 13 (2025); <https://doi.org/10.1021/acsoiginorgau.4c00072>
71. S. Jiang, Y. Zhang and J. Gong, *Environ. Sci. Nano*, **11**, 1332 (2024); <https://doi.org/10.1039/D3EN00983A>

72. G. Chen, S. Chen, J. Zhao, Z. Su and G. Liang, *Nano Res.*, **18**, 94907931 (2025); <https://doi.org/10.26599/NR.2025.94907931>
73. S.A. Ali, S. Sarkar and A.K. Patra, *ACS Appl. Mater. Interfaces*, **16**, 38061 (2024); <https://doi.org/10.1021/acsami.4c06647>
74. C. Imparato, A. Bifulco, B. Silvestri and G. Vitiello, *Catalysts*, **12**, 289 (2022); <https://doi.org/10.3390/catal12030289>
75. M. Konsolakis, S.A.C. Carabineiro, G.E. Marnellos, M.F. Asad, O.S.G.P. Soares, M.F.R. Pereira, J.J.M. Orfão and J.L. Figueiredo, *J. Colloid Interface Sci.*, **496**, 141 (2017); <https://doi.org/10.1016/j.jcis.2017.02.014>
76. X. Chen, J. Dai, G. Shi, L. Li, G. Wang and H. Yang, *J. Alloys Compd.*, **649**, 872 (2015); <https://doi.org/10.1016/j.jallcom.2015.05.096>
77. A.A. Oladipo and F.S. Mustafa, *Beilstein J. Nanotechnol.*, **14**, 291 (2023); <https://doi.org/10.3762/bjnano.14.26>
78. C. Murugan and A. Pandikumar, *ACS Appl. Energy Mater.*, **5**, 6618 (2022); <https://doi.org/10.1021/acsaem.1c04120>
79. Tarannum, V. Soni, M. Malhotra, A. Singh, V. Chaudhary, P. Singh, T. Ahmad, S. Kaya, C.M. Hussain and P. Raizada, *Environ. Res.*, **279**, 121670 (2025); <https://doi.org/10.1016/j.envres.2025.121670>
80. M.E. Malefane, P.J. Mafa, M. Managa, T.T.I. Nkambule and A.T. Kuvarega, *J. Phys. Chem. Lett.*, **14**, 1029 (2023); <https://doi.org/10.1021/acs.jpcclett.2c03387>
81. P.D. Walimbe, R. Kumar, A.K. Shringi, O. Keelson, H.A. Ouma and F. Yan, *Nanomaterials*, **14**, 1592 (2024); <https://doi.org/10.3390/nano14191592>
82. R. Murugan, A. Rebekah, C. Viswanathan, N. Ponpandian and J.A. Allen, *Colloids Surf. A Physicochem. Eng. Asp.*, **622**, 126612 (2021); <https://doi.org/10.1016/j.colsurfa.2021.126612>
83. S. Li, Y. Kang, C. Mo, Y. Peng, H. Ma and J. Peng, *Int. J. Mol. Sci.*, **23**, 14485 (2022); <https://doi.org/10.3390/IJMS232214485>
84. G. Varga, M. Kocsis, Á. Kukovecz, Z. Kónya, I. Djerdj, P. Sipos and I. Pálkó, *Mol. Catal.*, **493**, 111072 (2020); <https://doi.org/10.1016/j.mcat.2020.111072>
85. S. Mukai, Y. Yamada, S. Mukai and Y. Yamada, *Knowledge*, **3**, 1 (2022); <https://doi.org/10.3390/knowledge3010001>
86. R. Kusy and K. Grela, *Curr. Opin. Green Sustain. Chem.*, **38**, 100678 (2022); <https://doi.org/10.1016/j.cogsc.2022.100678>
87. M. Rezaei, A. Nezamzadeh-Ejehieh and A.R. Massah, *ACS Omega*, **9**, 6093 (2024); <https://doi.org/10.1021/acsomega.3c07560>
88. N. Goodarzi, Z. Ashrafi-Peyman, E. Khani and A.Z. Moshfegh, *Catalysts*, **13**, 1102 (2023); <https://doi.org/10.3390/catal13071102>
89. M. Smiljanić, S. Panić, M. Bele, F. Ruiz-Zepeda, L. Pavko, L. Gašparič, A. Kokalj, M. Gaberšček and N. Hodnik, *ACS Catal.*, **12**, 13021 (2022); <https://doi.org/10.1021/acscatal.2c03214>
90. U. Chadha, S.K. Selvaraj, H. Ashokan, S.P. Hariharan, V.M. Paul, V. Venkatarangan and V. Paramasivam, *Adv. Mater. Sci. Eng.*, **2022**, 1552334 (2022); <https://doi.org/10.1155/2022/1552334>
91. M.A. Ahmed, S.A. Mahmoud and A.A. Mohamed, *RSC Adv.*, **15**, 15561 (2025); <https://doi.org/10.1039/D4RA008780A>
92. Z. Saddique, M. Imran, A. Javaid, S. Latif, T.H. Kim, M. Janczarek, M. Bilal and T. Jesionowski, *Environ. Res.*, **229**, 115861 (2023); <https://doi.org/10.1016/j.envres.2023.115861>
93. C. Donga, R. Ratshiedana, A.T. Kuvarega, V.S. Vallabhapurapu, N. Masunga and P. Mbule, *Talanta*, **295**, 128318 (2025); <https://doi.org/10.1016/j.talanta.2025.128318>
94. E.M. Siedlecka, Application of Bismuth-Based Photocatalysts in Environmental Protection, In: Nanophotocatalysis and Environmental Applications. Environmental Chemistry for a Sustainable World, pp. 87–118, 2020; https://doi.org/10.1007/978-3-030-12619-3_4
95. H. Jiang, J. He, C. Deng, X. Hong and B. Liang, *Molecules*, **27**, 8698 (2022); <https://doi.org/10.3390/molecules27248698>
96. A.N. El-Shazly, M.A. Hamza and A.E. Shalan, in eds.: A.E. Shalan, A.S. Hamdy Makhlof and S. Lanceros-Méndez, Major Trends and Mechanistic Insights for the Development of TiO₂-Based Nanocomposites for Visible-Light-Driven Photocatalytic Hydrogen Production, In: Advances in Nanocomposite Materials for Environmental and Energy Harvesting Applications. Engineering Materials. Springer, Cham., pp. 771–794 (2022).
97. P. Sathishkumar, Photocatalysis for Energy and Environmental Applications, Springer (2024).
98. D. Zhang, T. Cong, L. Xia and L. Pan, *J. Mater. Sci.*, **54**, 7576 (2019); <https://doi.org/10.1007/s10853-019-03424-9>
99. N. Khanna, T. Chatterji, V. Yadav, T. Bhagat, S. Sharma and S. Pandey, in eds.: S. Pandey, E. Fosco-Kankeu and S. Pandit, Synergy of Bio-Chemical Processes for Photocatalytic and Photoelectrochemical Wastewater Treatment, In: Synergy of Bio-Chemical Processes for Photocatalytic and Photoelectrochemical Wastewater Treatment, Wiley, Chap. 8, p. 189 (2024); <https://doi.org/10.1002/9781394197903.ch8>
100. L. Zhang, Y. Meng, H. Shen, J. Li, C. Yang, B. Xie and S. Xia, *Appl. Surf. Sci.*, **567**, 150760 (2021); <https://doi.org/10.1016/j.apsusc.2021.150760>
101. C. Ma, Z. Xie, W.C. Seo, S.T. Ud Din, J. Lee, Y. Kim, H. Jung and W. Yang, *Appl. Surf. Sci.*, **565**, 150564 (2021); <https://doi.org/10.1016/j.apsusc.2021.150564>
102. J. Bai, B. Zhang, T. Xiong, D. Jiang, X. Ren, P. Lu and M. Fu, *J. Alloys Compd.*, **887**, 161297 (2021); <https://doi.org/10.1016/j.jallcom.2021.161297>
103. G.X. Castillo-Cabrera, P.J. Espinoza-Montero, P. Alulema-Pullupaxi, J.R. Mora and M.H. Villacís-García, *Front Chem.*, **10**, 900622 (2022); <https://doi.org/10.3389/fchem.2022.900622>
104. I.M. Kobasa and G.P. Tarasenko, *Theor. Exp. Chem.*, **38**, 255 (2002); <https://doi.org/10.1023/A:1020519932567>
105. H. Xue, X. Lin, Q. Chen, Q. Qian, S. Lin, X. Zhang, D.-P. Yang and L. Xiao, *Nanoscale Res. Lett.*, **13**, 114 (2018); <https://doi.org/10.1186/s11671-018-2522-5>
106. J. Wang, Y. Lin, W. Lv, Y. Yuan, S. Guo and W. Yan, *Molecules*, **28**, (2023); <https://doi.org/10.3390/MOLECULES28186464/S1>
107. R. Kumari, N. Chandrakar, D. Choudhary, D. Guin and C.S.P. Tripathi, *Environ. Sci. Pollut. Res. Int.*, **32**, 11535 (2025); <https://doi.org/10.1007/s11356-025-36365-9>
108. T. Nawaz, M.B. Tahir, M. Sagir, K. Shahzad, A.M. Ali and H. Alrobei, *Ceram. Int.*, **48**, 11779 (2022); <https://doi.org/10.1016/j.ceramint.2022.01.037>
109. K. Liu, T. Fu, L. Wang, J. Yan, J. Sun, J. Zhang, X. Wei, Z. Tong and H. Zhang, *Sep. Purif. Technol.*, **323**, 124427 (2023); <https://doi.org/10.1016/j.seppur.2023.124427>
110. A. Karimirahnama and M. Mozaffarian, *Sci. Rep.*, **15**, 41551 (2025); <https://doi.org/10.1038/s41598-025-25451-0>
111. L. Dashairya, M. Sharma, S. Basu and P. Saha, *J. Alloys Compd.*, **735**, 234 (2018); <https://doi.org/10.1016/j.jallcom.2017.11.063>
112. M. Ashfaq, A. Ali, N.K. Abbood, S. Panchal, N. Akram, M. Saeed, O.P. Doshi, F. Ali, S. Muhammad, M.Y. Sameeh and A.N. Nazar, *Water*, **15**, 3182 (2023); <https://doi.org/10.3390/w15183182>
113. R. Balint, M. Bartoli, P. Jagdale, A. Tagliaferro, A. Memon, M. Rovere and M. Martin, *Toxics*, **9**, 158 (2021); <https://doi.org/10.3390/toxics9070158>
114. A. Lathe and A.M. Palve, *J. Hazard. Mater. Adv.*, **12**, 100333 (2023); <https://doi.org/10.1016/j.hazadv.2023.100333>
115. J. Fu, B. Zhu, C. Jiang, B. Cheng and J. Yu, *Small*, **13**, 1603938 (2017); <https://doi.org/10.1002/sml.201603938>
116. C.B. Ong, L.Y. Ng and A.W. Mohammad, *Renew. Sustain. Energy Rev.*, **81**, 536 (2018); <https://doi.org/10.1016/j.rser.2017.08.020>
117. J. Schneider, M. Matsuoka, M. Takeuchi, J. Zhang, Y. Horiuchi, M. Anpo and D.W. Bahnemann, *Chem. Rev.*, **114**, 9919 (2014); <https://doi.org/10.1021/cr5001892>
118. X. Chen, N. Li, Z. Kong, W.J. Ong and X. Zhao, *Mater. Horiz.*, **5**, 9 (2018); <https://doi.org/10.1039/C7MH00557A>
119. L. Zhang, W. Wang, J. Yang, Z. Chen, W. Zhang, L. Zhou and S. Liu, *Appl. Catal. A Gen.*, **308**, 105 (2006); <https://doi.org/10.1016/j.apcata.2006.04.016>

120. R.I. Cornejo-Bravo, A.G. López and H.M. Hernández, *Chem. Soc. Rev.*, **49**, 3224 (2020); <https://doi.org/10.1039/C9CS00283A>
121. H. Tang, G. Meng, J. Xiang, A. Mahmood, G. Xiang, SanaUllah, Y. Liu and G. Huang, *Front. Plant Sci.*, **13**, 1011945 (2022); <https://doi.org/10.3389/fpls.2022.1011945>
122. B. Barbu, *C&EN Global Enterprise*, **102**, 28 (2024); <https://doi.org/10.1021/cen-10205-cover>
123. G. Hu, H. Liu, C. Chen, P. He, J. Li and H. Hou, *Sci. Total Environ.*, **845**, 157211 (2022); <https://doi.org/10.1016/j.scitotenv.2022.157211>
124. S. Pérez, A. Vázquez-García, A. Gutiérrez-Pérez, M.T. Ayala-Ayala, M. Boujnah, J. Tapia-P, J.A. Díaz-Real and J. Muñoz-Saldaña, *Environ. Res.*, **289**, 123384 (2026); <https://doi.org/10.1016/j.envres.2025.123384>
125. G.S. Kamble, T.S. Natarajan, S.S. Patil, M. Thomas, R.K. Chougale, P.D. Sanadi, U.S. Siddharth and Y.-C. Ling, *Nanomaterials*, **13**, 1528 (2023); <https://doi.org/10.3390/nano13091528>
126. M.A. Reynolds, *Energy Fuels*, **35**, 15285 (2021); <https://doi.org/10.1021/acs.energyfuels.1c02039>
127. L. Dong, P.N. Liu and N. Lin, *Acc. Chem. Res.*, **48**, 2765 (2015); <https://doi.org/10.1021/acs.accounts.5b00160>
128. X. Jaramillo-Fierro, G. Cuenca, X. Jaramillo-Fierro and G. Cuenca, *Int. J. Mol. Sci.*, **25**, 4367 (2024); <https://doi.org/10.3390/ijms25084367>
129. C. Nicosia and J. Huskens, *Mater. Horiz.*, **1**, 32 (2014); <https://doi.org/10.1039/C3MH00046J>
130. M. Arif, M. Zhang, B. Qiu, J. Yao, Q. Bu, A. Ali, T. Muhmood, I. Hussian, X. Liu, B. Zhou and X. Wang, *Appl. Surf. Sci.*, **543**, 148816 (2021); <https://doi.org/10.1016/j.apsusc.2020.148816>
131. X. Chen, P.V. Kamat, C. Janáky and G.F. Samu, *ACS Energy Lett.*, **9**, 3187 (2024); <https://doi.org/10.1021/acsenerylett.4c00736>
132. S.J. Lee, H. Jang and D.N. Lee, *Nanoscale Adv.*, **5**, 5165 (2023); <https://doi.org/10.1039/D3NA00163F>
133. V. Gacha, C. Ros, X. Garcia, J. Llorca, J. Martorell and D. Raptis, *Appl. Mater. Today*, **40**, 102415 (2024); <https://doi.org/10.1016/j.apmt.2024.102415>
134. A.A.H. Abdellatif, M.A.H. Mostafa, H. Konno and M.A. Younis, *3 Biotech*, **14**, 274 (2024); <https://doi.org/10.1007/s13205-024-04118-z>
135. J. Li, Y. Wang, Y. Guo, S. Zhang and Y. Kuai, *Colloids Surf. A Physicochem. Eng. Asp.*, **729**, 138931 (2026); <https://doi.org/10.1016/j.colsurfa.2025.138931>
136. S. Hosny, G.A. Gaber, M.S. Ragab, M.A. Ragheb, M. Anter and L.Z. Mohamed, *Arab. J. Sci. Eng.*, **2025**, 13667 (2025); <https://doi.org/10.1007/s13369-025-10612-0>
137. B. Mughal, S.Z.J. Zaidi, X. Zhang and S.U. Hassan, *Appl. Sci.*, **11**, 2598 (2021); <https://doi.org/10.3390/app11062598>
138. E. Milan, Master's Thesis, Continuous Photocatalytic Treatment of Selenate from Mine-Impacted Water and Brine Using an Annular Photoreactor, University of Toronto, Toronto, Canada (2025).
139. M. Hassnain, A. Ali, M.R. Azhar, A. Abutaleb and M. Mubashir, *Glob. Chall.*, **9**, 2500035 (2025); <https://doi.org/10.1002/gch2.202500035>
140. M. Shakibaie, H. Forootanfar, A. Ameri, M. Adeli-Sardou, M. Jafari and H.R. Rahimi, *IET Nanobiotechnol.*, **12**, 653 (2018); <https://doi.org/10.1049/iet-nbt.2017.0295>
141. F. Feola, A. Segura, I. Galain, I. Aguiar, I. Machado, M. Pistón and M.E.P. Barthaburu, *J. Nanopart. Res.*, **27**, 272 (2025); <https://doi.org/10.1007/s11051-025-06466-0>
142. A. Chowdhury and M. Ghosh, *Front. Nanotechnol.*, **7**, 1666431 (2025); <https://doi.org/10.3389/fnano.2025.1666431>
143. E. Zayerzadeh and M.K. Koochi, *Nanomed. Res. J.*, **9**, 339 (2024); <https://doi.org/10.22034/nmrj.2024.04.001>
144. M. Scaccaglia, L. Verderi, L. Manini, M. Rega, S. Pinelli, C. Bacci, G. Pelosi and F. Bisceglie, *J. Inorg. Biochem.*, **274**, 113092 (2026); <https://doi.org/10.1016/j.jinorgbio.2025.113092>
145. N. Mpongwana and S. Rathilal, *Water*, **14**, 1550 (2022); <https://doi.org/10.3390/w14101550>
146. D.A. Henry and W.D. Birch, *Mineral. Mag.*, **86**, 606 (2022); <https://doi.org/10.1180/mgm.2022.11>